

# Galactic Archaeology

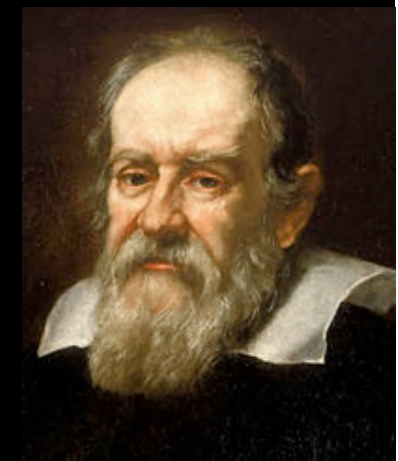
Stars are direct tracers of the Early Universe

low mass stars

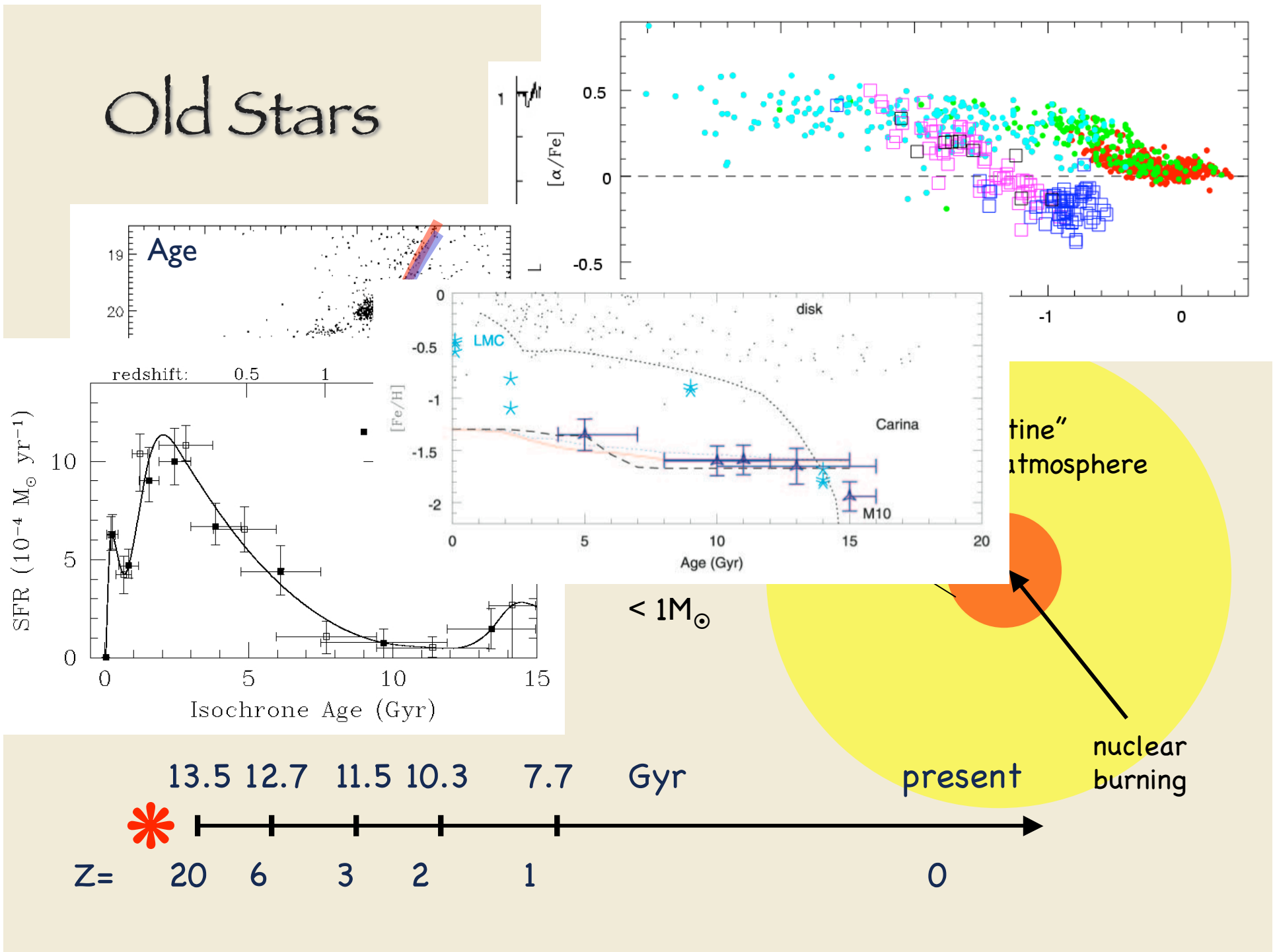


# The Closest Galaxy

...congeries  
stellularum...

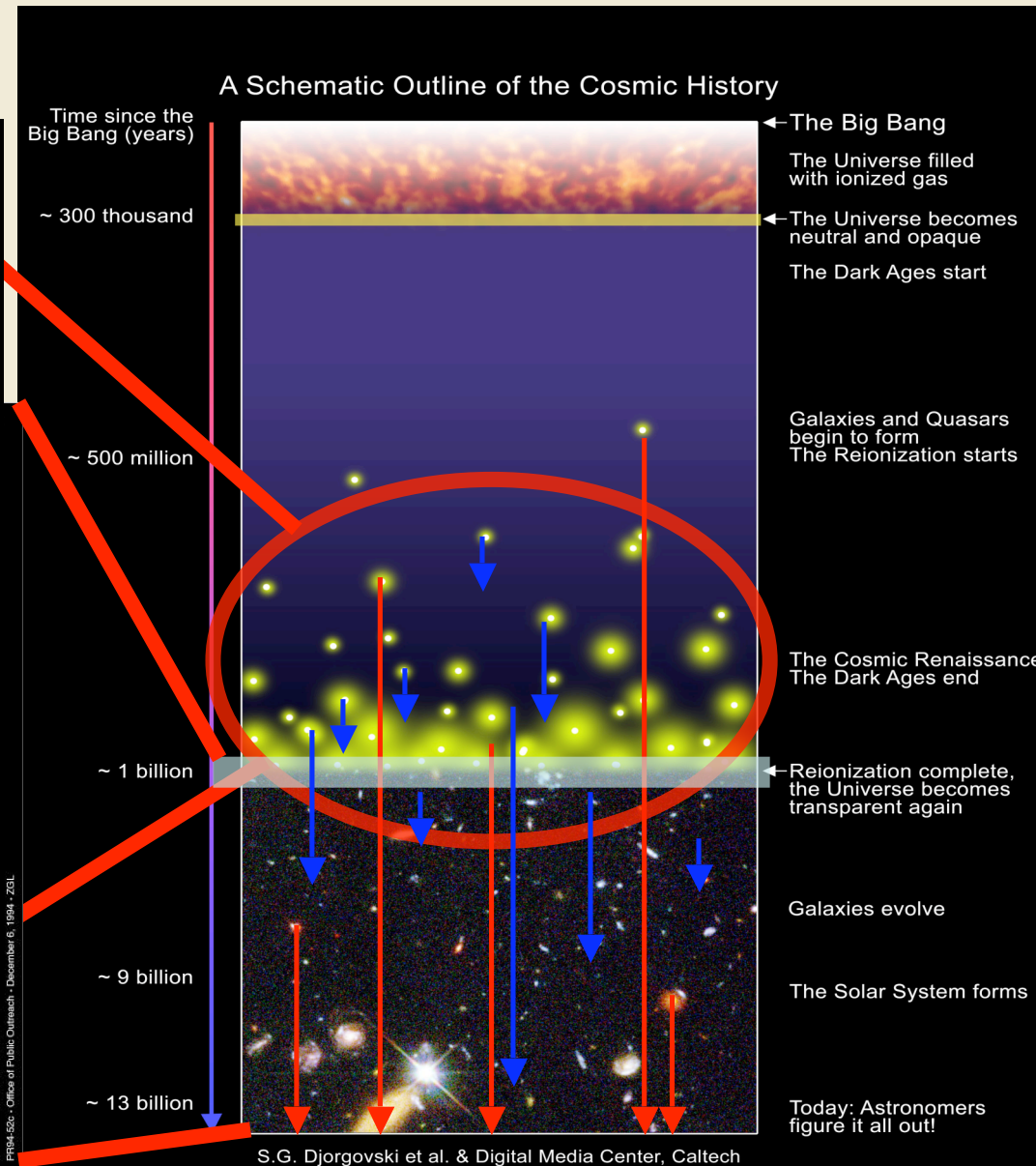
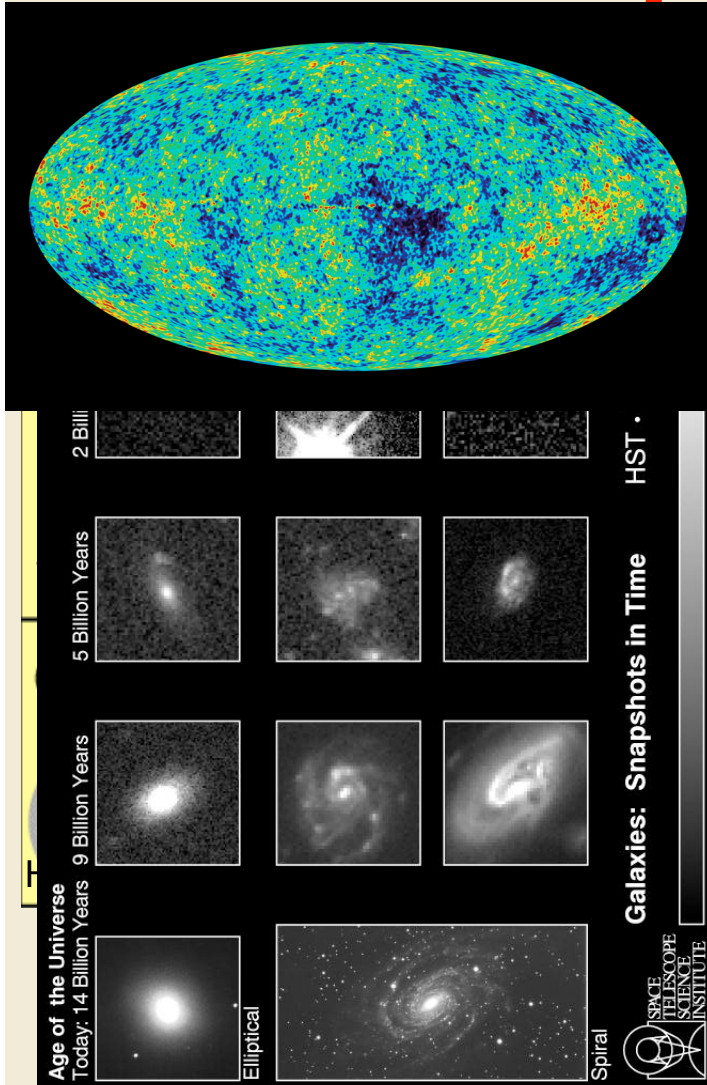


# Old Stars

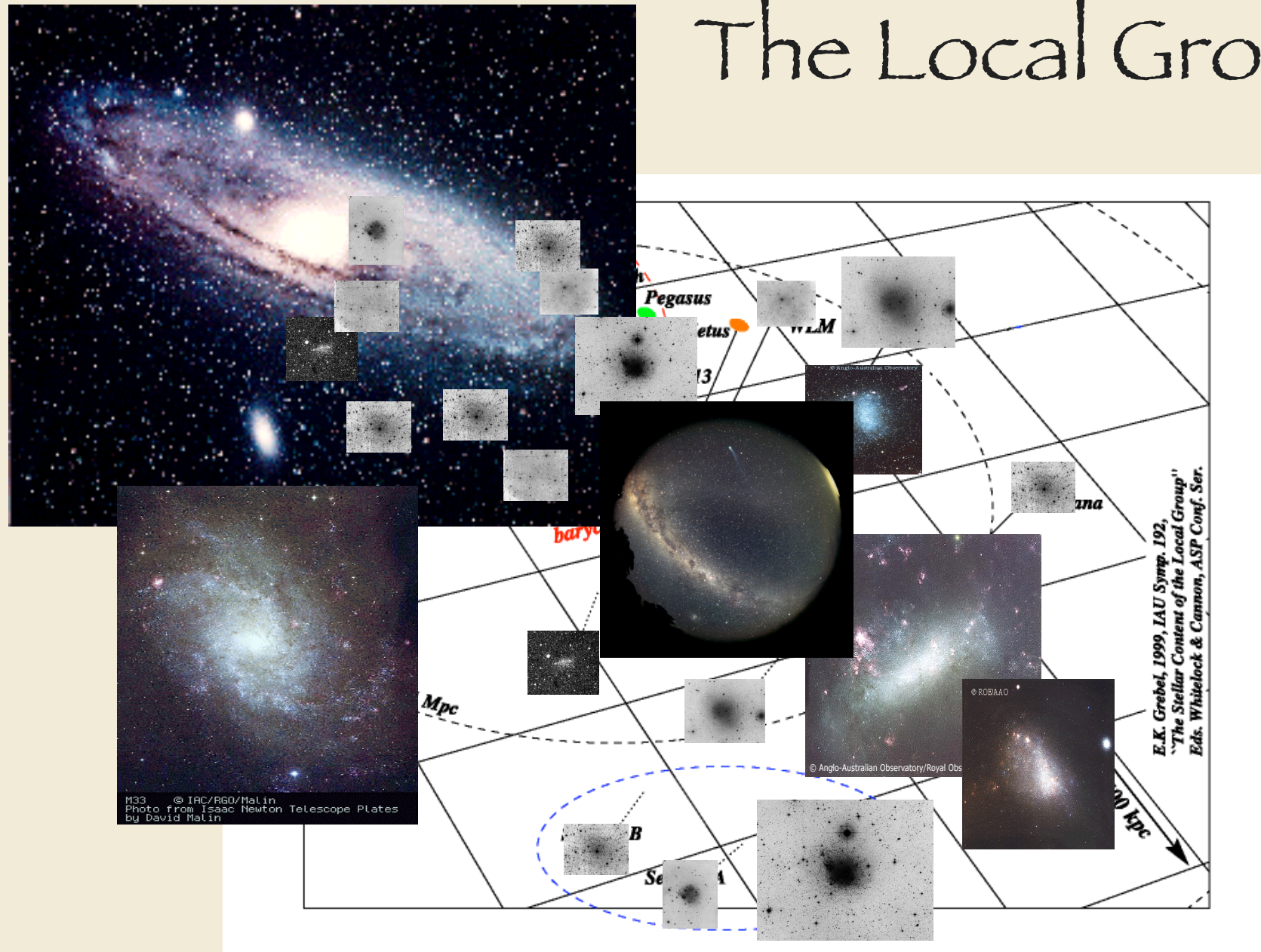


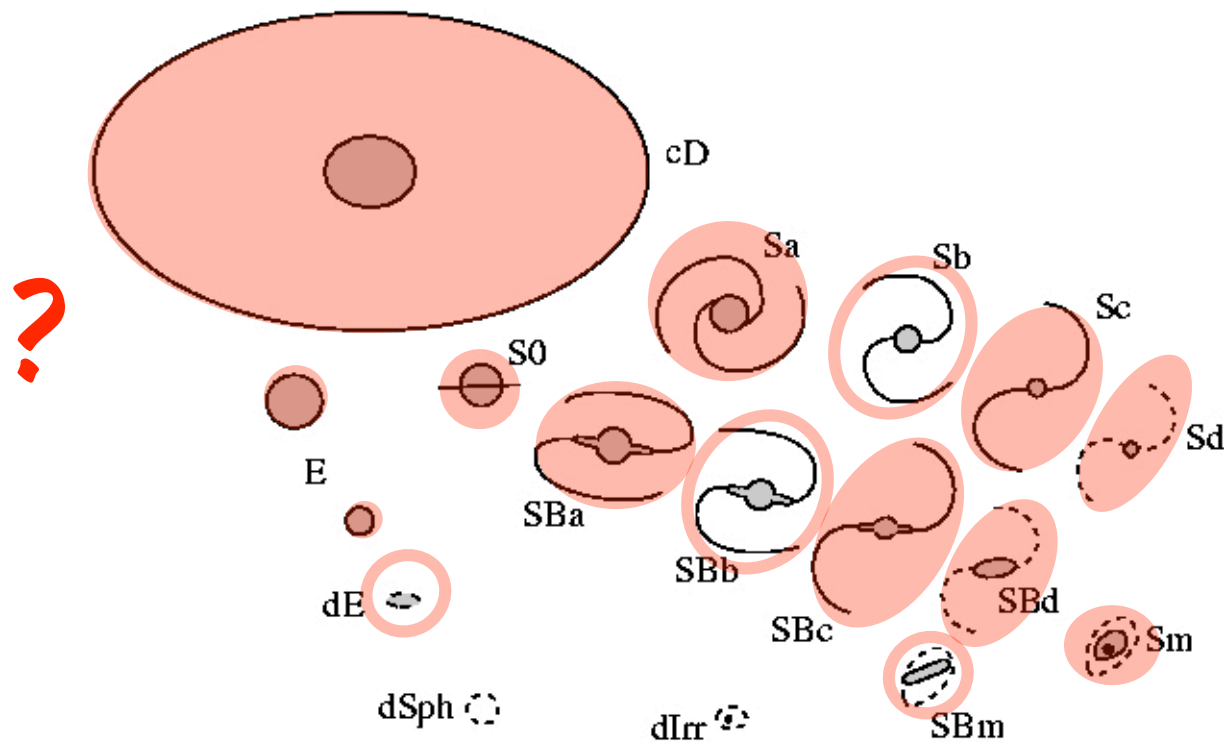
# Cosmic History

## Big Bang



# The Local Group







# Stellar Pops DRM

- ★ Imaging
- ★ Low resolution spectroscopy ( $R \approx 5000$ )
- ★ High Resolution spectroscopy ( $R \geq 20000$ )

# Why Optical?

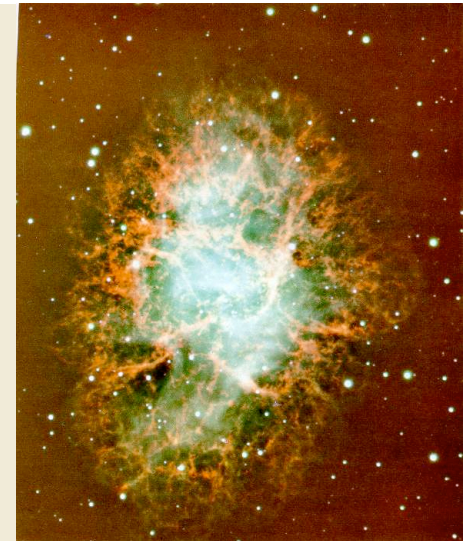
- ★ For low metallicity stars most of the observable lines which are easy to interpret are at optical wavelengths (and mostly quite blue, < 680nm).
- ★ Higher diffraction-limited spatial resolution in the optical (a factor of 3 to 4 higher than in the infrared, corresponding to magnitudes of depth in crowded fields) - most stellar population applications are confusion-limited rather than sky-background or photon limited and typically attainable depths are 7 magnitudes fainter in V than in K.
- ★ The derivation of stellar parameters such as age and metallicity is more robust in the optical than in the near-IR.

## HIGH RESOLUTION SPECTROSCOPY:

*Stars are direct tracers of the early universe*

# Chemical Tagging

- Light Elements – e.g., O Na Mg Al  
tracers of deep mixing abundances patterns  
(globular clusters versus field stars)
- $\alpha$ - Elements – e.g., O Mg Si Ca Ti  
dominated by products of Supernovae II
- Iron-peak Elements e.g., V Cr Mn Co Ni Cu Zn  
explosive nucleosynthesis (supernovae I)
- Heavy Elements ( $Z > 30$ )  
mix of r- and s- process elements  
e.g., s-process e.g., Ba, La (stellar winds)  
r-process e.g., Eu



e.g., McWilliam 1997

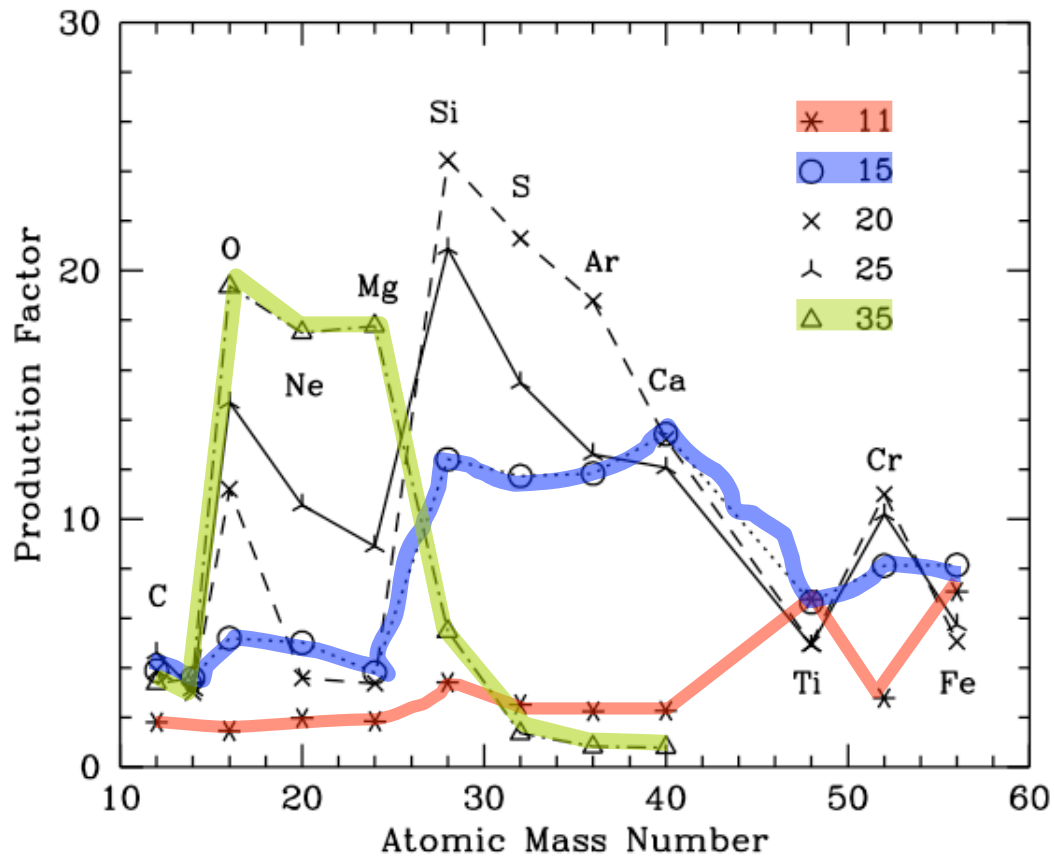
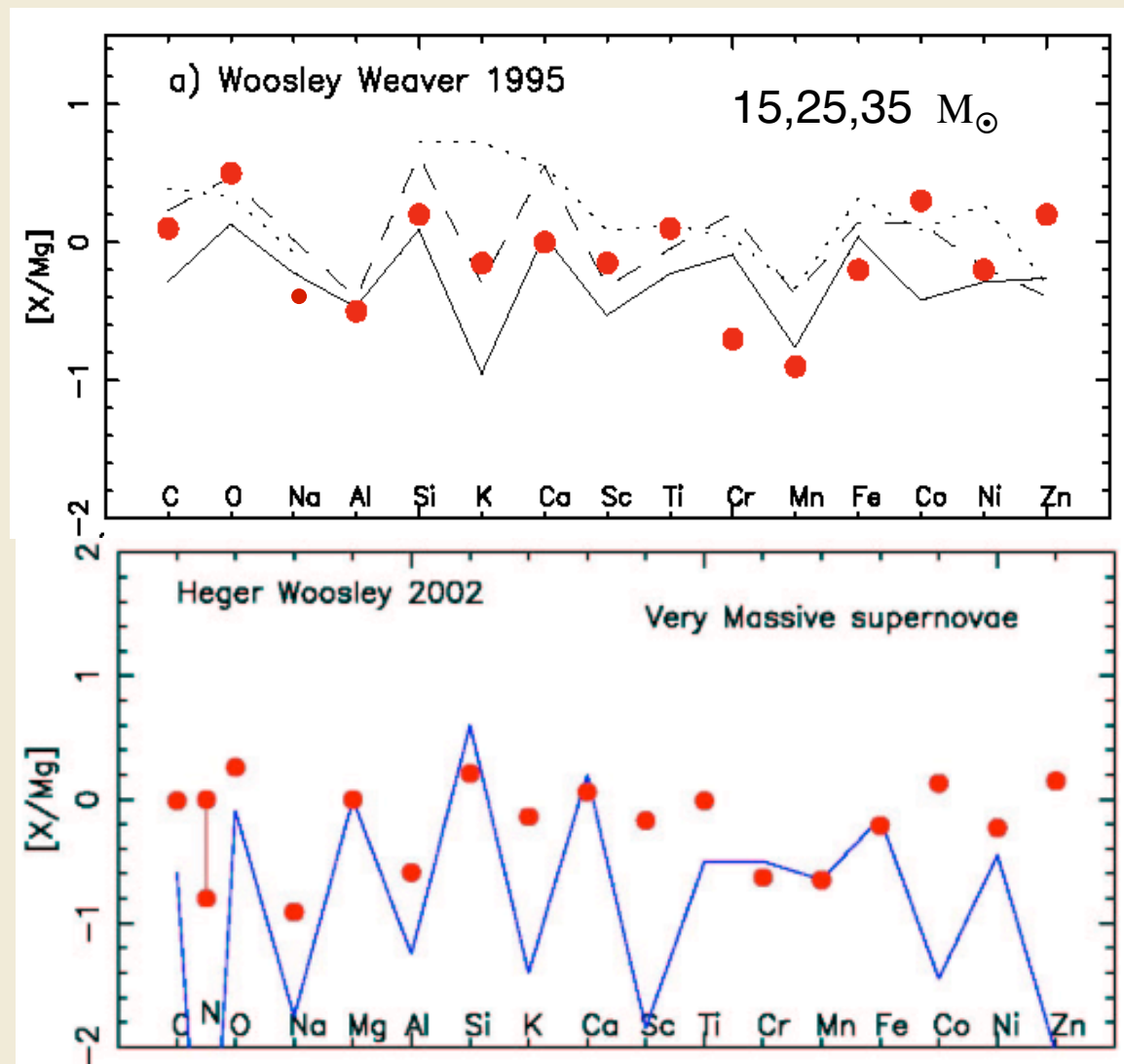
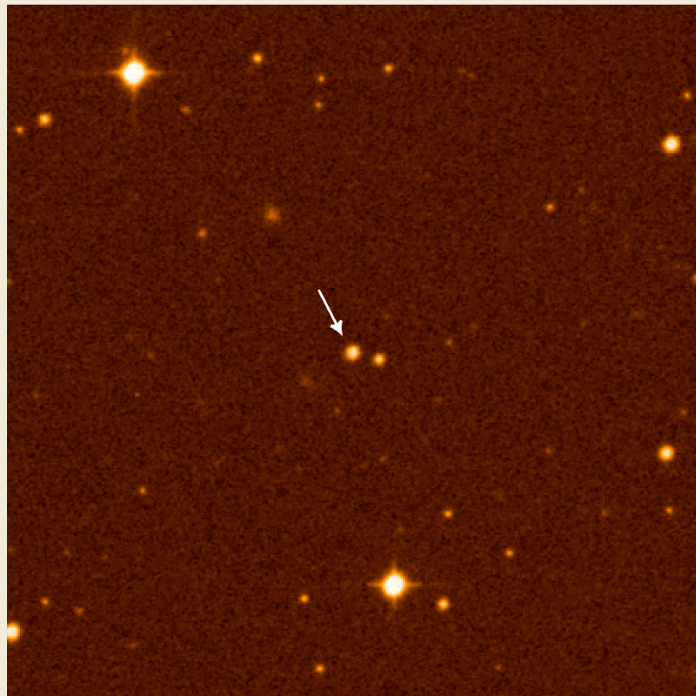


**Figure 6** Production factors from models of SN II by Woosley & Weaver (1995). Ejected element abundances for various progenitor masses are indicated by *connected symbols*; O and Mg are produced in large quantities at high mass ( $\sim 35 M_{\odot}$ ) but not in the lower mass (15–25  $M_{\odot}$ ) SN, which are responsible for most of the Si and Ca production. None of the models give significant enhancements of Ti relative to Fe, contrary to observations of stars in the Galactic bulge and halo. Note that production factor is defined as the ratio of the mass fraction of an isotope in the SN ejecta, divided by its corresponding mass fraction in the Sun. The mass of the progenitor making the indicated elements is given in the key in the upper right.

# Constraining early chemical enrichment



# HE0107-5240: The Most ancient object we know of ?



The Very Metal-Deficient Star HE 0107-5240

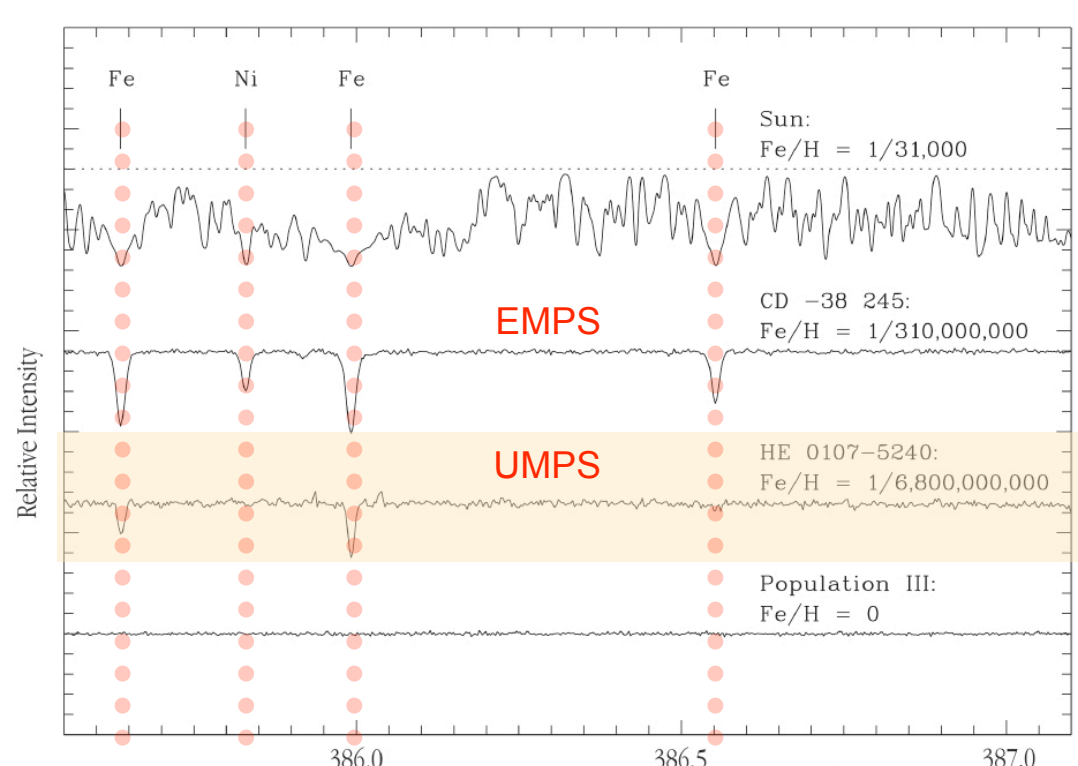
ESO PR Photo 25a/02 (30 October 2002)

© European Southern Observatory



HE 0107-5240

$[\text{Fe}/\text{H}] \approx -5.4$



Spectra of Stars with Different Metal Content

ESO PR Photo 25b/02 (30 October 2002)

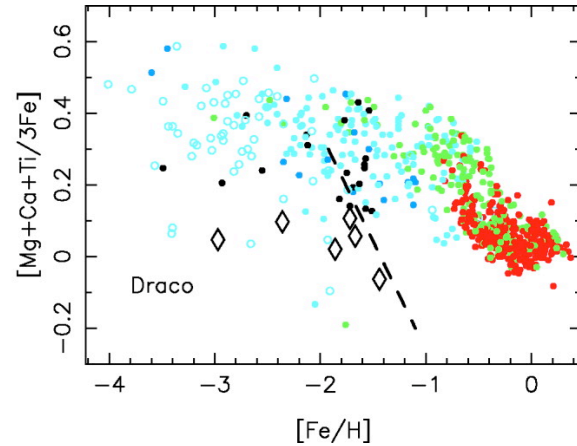
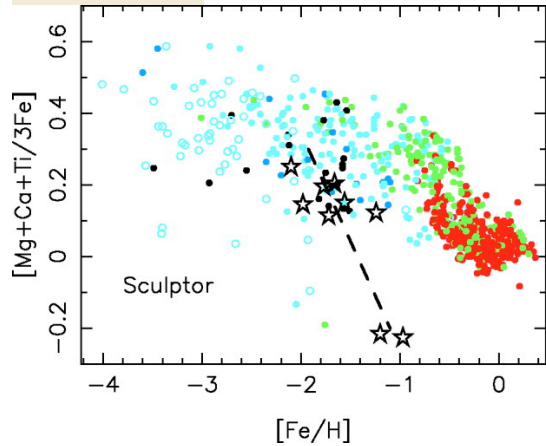
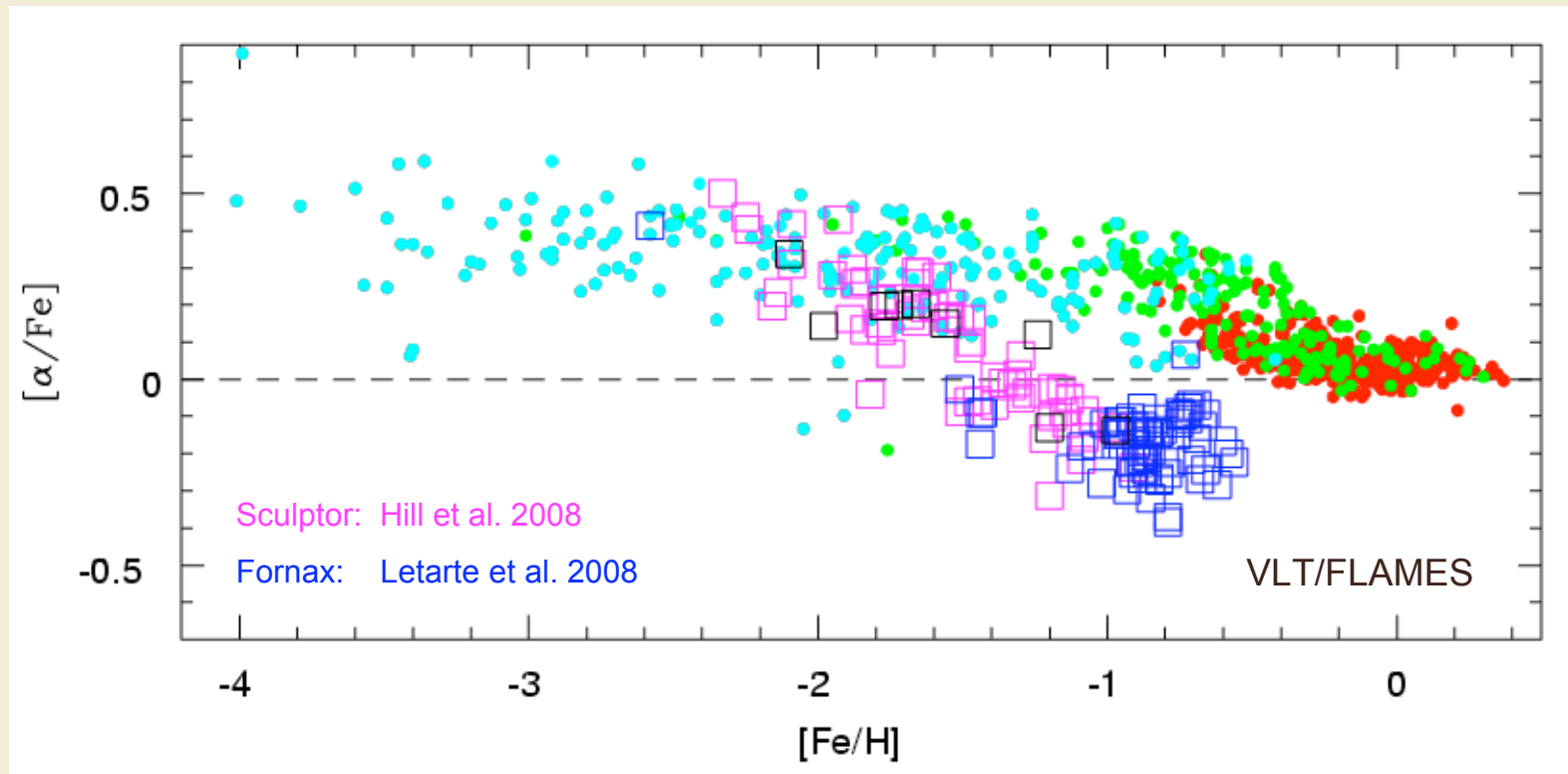
© European Southern Observatory



Christlieb & HES

# Alpha Abundances in dSph

Hard to make any component of MW from dwarf satellites...



Shetrone et al. 2001, 2003;  
Tolstoy et al. 2003



# HR spectroscopy cases:

R~20000 resolution spectroscopy in the visible and near-infrared, to measure detailed abundances of metals in a variety of stars, to probe the source and timescales of metal enrichment in galaxies. Examples of prominent science cases include:

**-Detailed abundances in old red giants at the edge of the Local-Group** (dwarf Irregular galaxies, isolated dwarf spheroidal galaxies, M31, M32, M33) to unravel the chemical enrichment timescale and nature within range of galaxy types.

**-Detailed abundances of B-A super-giants in spiral galaxies outside the Local Group,** out to the Sculptor or M82 groups (2Mpc away). The 0.2" resolution provided by the GLAO corresponds to 0.6 pc at the distance of M31 and 1.8 pc at the distance of the Sculptor group, it will be perfectly suited for this study.

**-Detailed abundances of metal poor dwarf & giants stars in the halo of MW & M31**  
there are a number of lines which are too weak to be detected with present day instrumentation (e.g., Li, U, Be, r-process elements).

The spectrograph extension towards visible wavelengths will have a large impact in this science case, since most of the strong metal-lines are located in the visible. On the other hand, detailed abundances in metal-rich populations (such as bulges and young stellar disks) can be measured in the infrared.

Stell param

[Fe/H]<-5.

R-process

compiled by Christlieb & Hill

| Quantity                      | Indicator                        | Minium $R = \lambda/\Delta\lambda$ |         |            | Minium S/N per pixel |         |            | Notes |
|-------------------------------|----------------------------------|------------------------------------|---------|------------|----------------------|---------|------------|-------|
|                               |                                  | G/-5.2                             | SG/-5.4 | r-II giant | G/-5.2               | SG/-5.4 | r-II giant |       |
| $T_{\text{eff}}$              | H $\alpha$                       | 40,000                             | 40,000  | 40,000     | 150                  | 150     | 150        |       |
| $\log g$                      | Fe I/Fe II                       | 20,000                             | 20,000  | 20,000     |                      |         |            | 1     |
| $\log g$                      | Ca I/Ca II                       | 20,000                             | 20,000  | 20,000     |                      |         |            |       |
| $\xi_{\text{micr}}$           | Fe I                             | 40,000                             | 60,000  | 20,000     | 50                   | 200     | 30         | 2     |
| $\log \epsilon(^7\text{Li})$  | 'Li 6707.76 Å                    | —                                  | 40,000  | —          | —                    | 120     | —          | 3     |
| $\log \epsilon(\text{C})$     | CH                               | 20,000                             | 20,000  | 20,000     |                      |         |            |       |
| $\log \epsilon(\text{N})$     | CN                               | 20,000                             | 20,000  | 20,000     |                      |         |            |       |
| $\log \epsilon(\text{N})$     | NH 3360 Å                        | 40,000                             | 20,000  |            | 70                   | 50      |            |       |
| $\log \epsilon(\text{O})$     | OH 3100 Å                        | 40,000                             | 40,000  | 40,000     | 30                   | 40      |            |       |
| $^{12}\text{C}/^{13}\text{C}$ | $^{12}\text{CH}, ^{13}\text{CH}$ | 40,000                             | —       | 40,000     | 100                  |         |            |       |
| $\log \epsilon(\text{Mg})$    | Mg I 3838.29 Å                   | 40,000                             | 40,000  | 20,000     | 40                   | 40      | 50         |       |
| $\log \epsilon(\text{Mg})$    | Mg I 5183.60 Å                   | 40,000                             | 40,000  | 20,000     | 100                  | 60      | 50         |       |
| $\log \epsilon(\text{Ca})$    | Ca I 4226.73 Å                   | 40,000                             | 60,000  | 20,000     | 60                   | 370     | 50         |       |
| $\log \epsilon(\text{Ca})$    | Ca II                            |                                    |         | 20,000     |                      |         | 50         |       |
| $\log \epsilon(\text{Ti})$    |                                  |                                    |         | 20,000     |                      |         | 50         |       |
| $\log \epsilon(\text{Mn})$    |                                  |                                    |         | 20,000     |                      |         | 50         |       |
| $\log \epsilon(\text{Fe})$    | Fe I 3859.91 Å                   | 40,000                             | 40,000  | 20,000     | 20                   | 200     | 50         |       |
| $\log \epsilon(\text{Fe})$    | Fe II 3227.74 Å                  | 40,000                             | —       | 20,000     |                      |         | 50         |       |
| $\log \epsilon(\text{Co})$    | Co I                             |                                    |         | 20,000     |                      |         | 50         |       |
| $\log \epsilon(\text{Ni})$    |                                  |                                    |         | 20,000     |                      |         | 50         |       |
| $\log \epsilon(\text{Zn})$    |                                  |                                    |         | 20,000     |                      |         | 50         |       |
| $\log \epsilon(\text{Sr})$    | Sr II 4077.72 Å                  | —                                  | 40,000  | 20,000     | —                    | 200     | 30         |       |
| $\log \epsilon(\text{Y})$     |                                  | —                                  | —       | 20,000     |                      |         | 50         |       |
| $\log \epsilon(\text{Zr})$    |                                  | —                                  | —       | 20,000     |                      |         | 50         |       |
| $\log \epsilon(\text{Ba})$    | Ba II 4554.03 Å                  | —                                  | —       | 20,000     |                      |         | 30         |       |
| $\log \epsilon(\text{La})$    |                                  | —                                  | —       | 20,000     |                      |         | 50         |       |
| $\log \epsilon(\text{Eu})$    | Eu II 4129.73 Å                  | —                                  | —       | 20,000     |                      |         | 30         |       |
| $\log \epsilon(\text{Os})$    |                                  | —                                  | —       |            |                      |         |            |       |
| $\log \epsilon(\text{Ir})$    |                                  | —                                  | —       |            |                      |         |            |       |
| $\log \epsilon(\text{Pb})$    |                                  | —                                  | —       |            |                      |         |            |       |
| $\log \epsilon(\text{Th})$    |                                  | —                                  | —       | 40,000     | —                    | —       | 50         |       |
| $\log \epsilon(\text{U})$     |                                  | —                                  | —       | 75,000     | —                    | —       | 150        |       |

Notes.

1 – Detection of at least one Fe II line required.

2 – Detection of at least a couple of Fe I lines required.

3 – Assuming an abundance of  $\log \epsilon(^7\text{Li}) = 2.2$ .

Table 3: Data quality requirements for spectroscopic analyses of metal-poor stars.

# HR spectroscopy: requirements

MOS: > 100 stars per galaxy; 0.48-2.2 $\mu$ m; R~20000

SOS: 10-100 stars per local galaxy; 300-700nm; R~40000 (min)

$M_i > -4$

# The Effect of Resolution

Integration  
time twice as  
long for H9

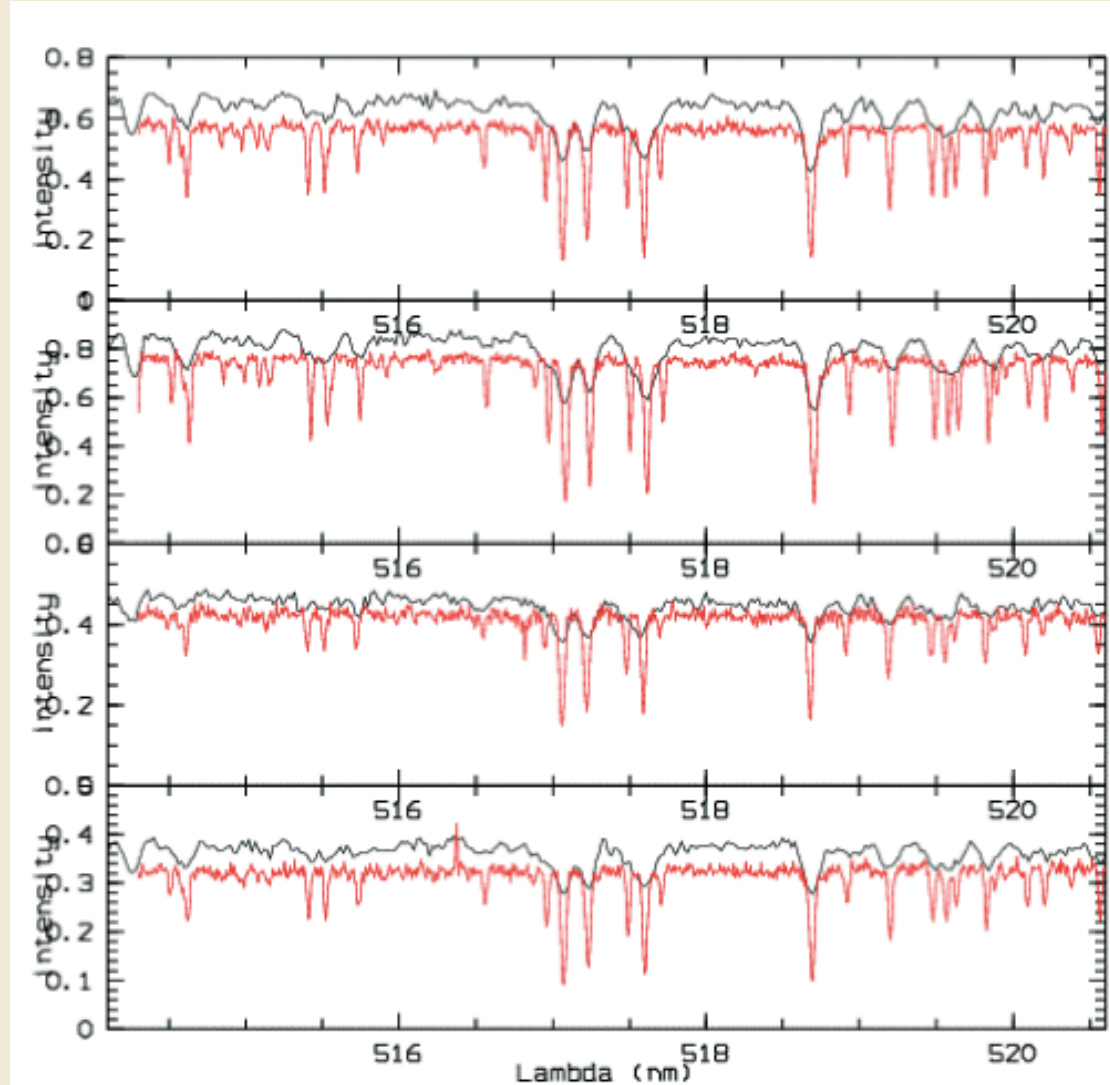
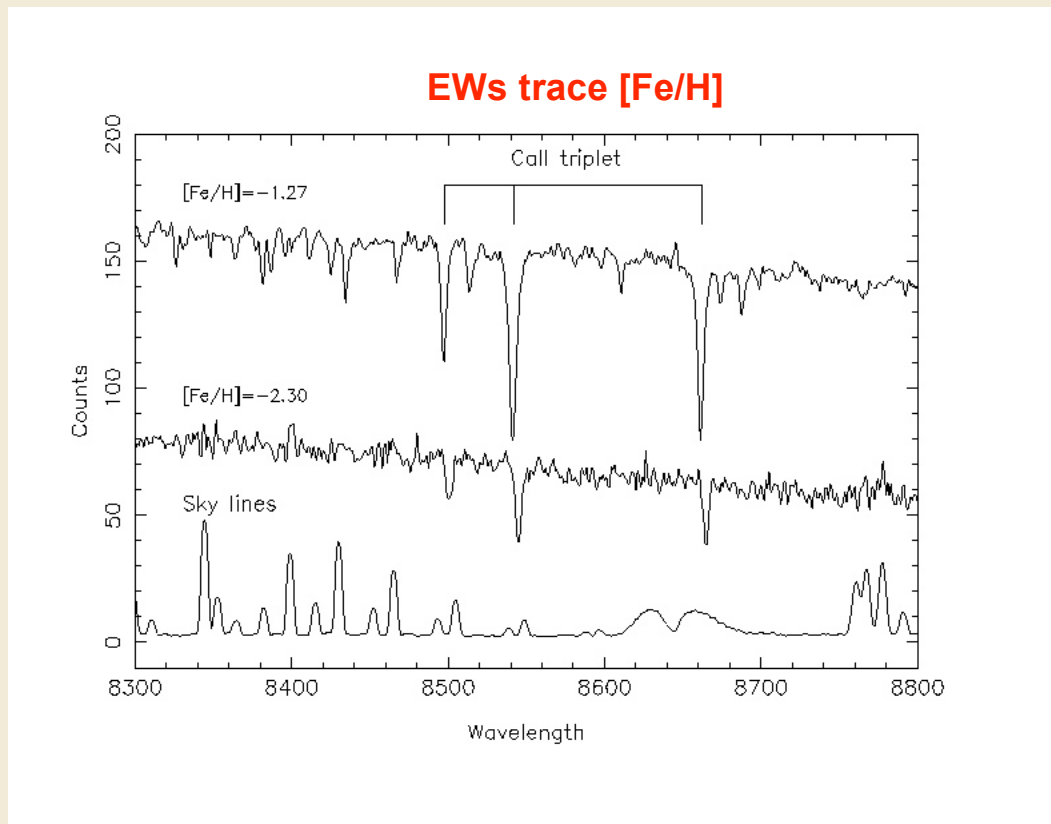


Figure 15: **GIRAFFE** Low (L4, black lines) and High (H9, red lines) resolution spectra of 4 giants belonging to the Globular Cluster NGC 6809

H9,  $R \sim 26000$

L4,  $R \sim 6000$

# Low Resolution Stellar Spectroscopy: the Ca II Triplet

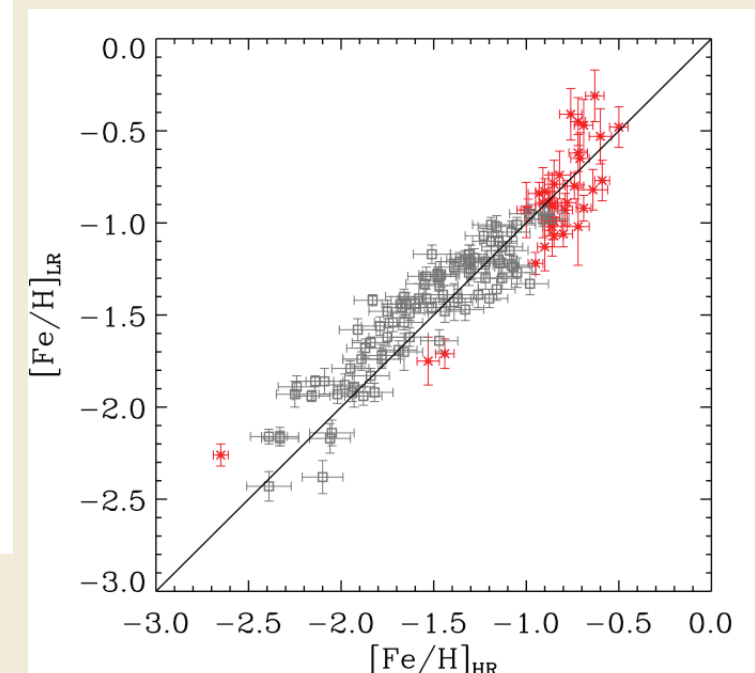


Also MgB region  $\lambda\lambda 440-550\text{nm}$

FORS / FLAMES

$\lambda\lambda 820-920\text{nm}$

$R \sim 6\,000$



Battaglia et al. 2008

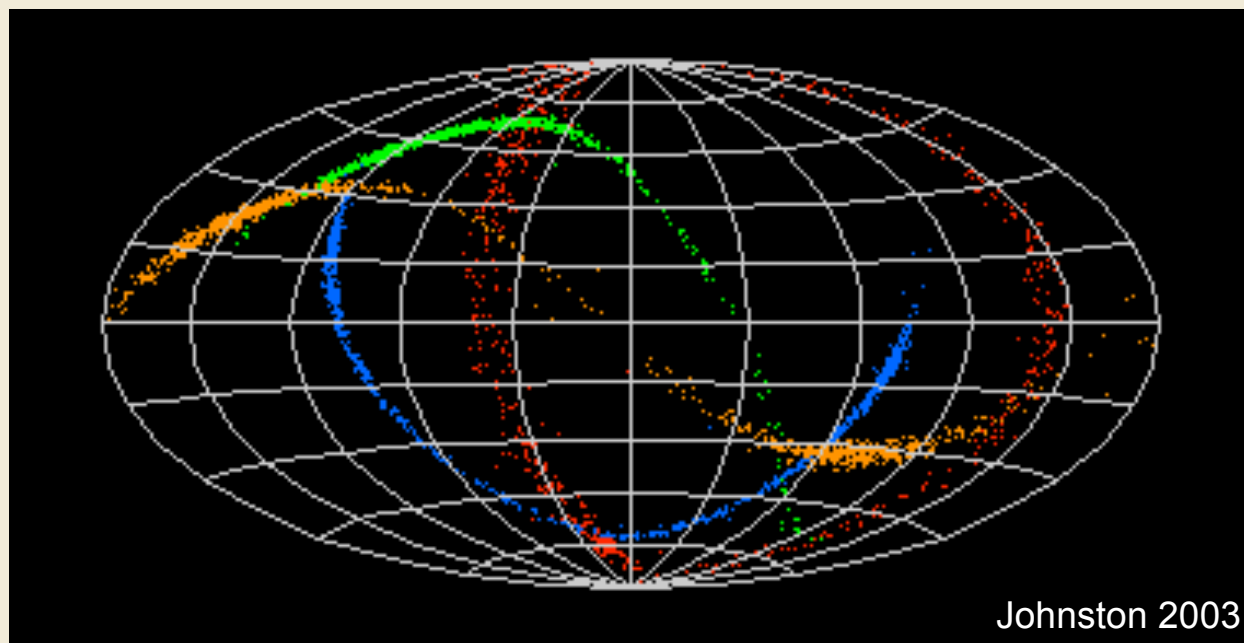
## LOW RESOLUTION SPECTROSCOPY:

Stars trace kinematics (mass) & chemical evolution

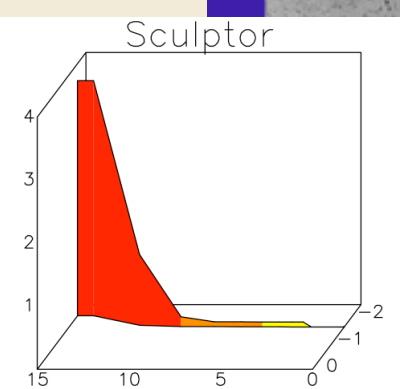
# Looking for Evidence on small scales...

Is the outer halo filled with tidal streams from disrupted dwarf galaxies that remain coherent in phase space?

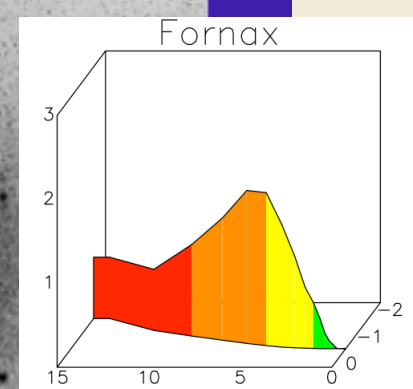
(Johnston et al. 1996; Helmi & White 1999 etc...)



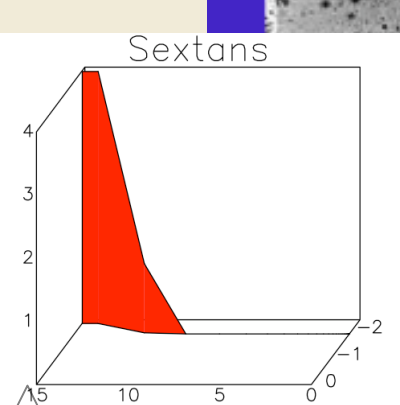
# Local dSph studied with FLAMES



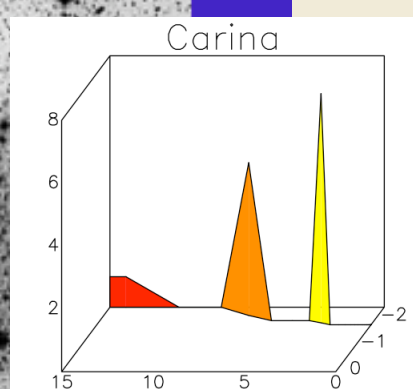
*Sculptor*



*Fornax*



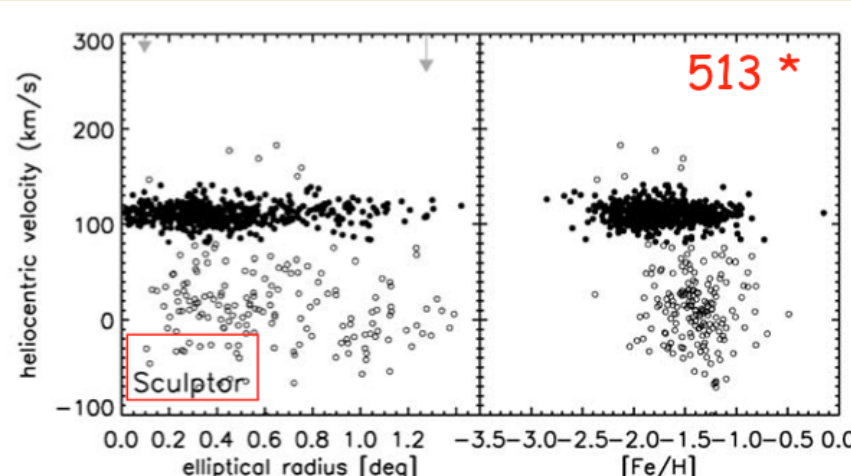
*Sextans*



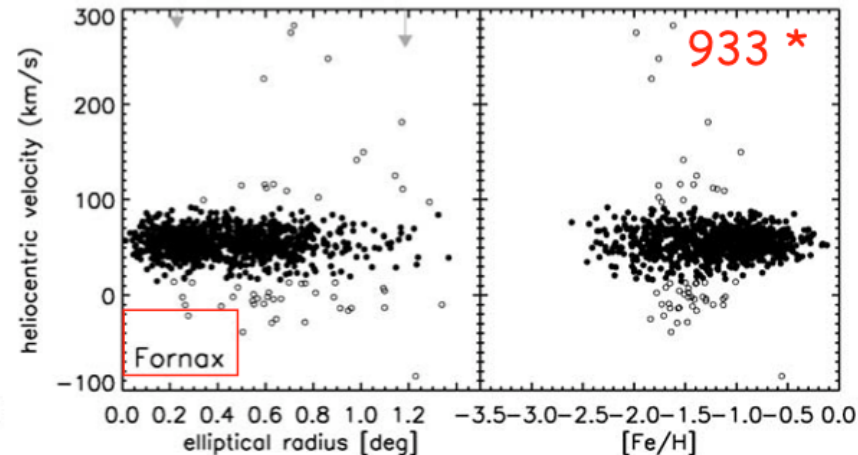
*Carina*

DAR  
★

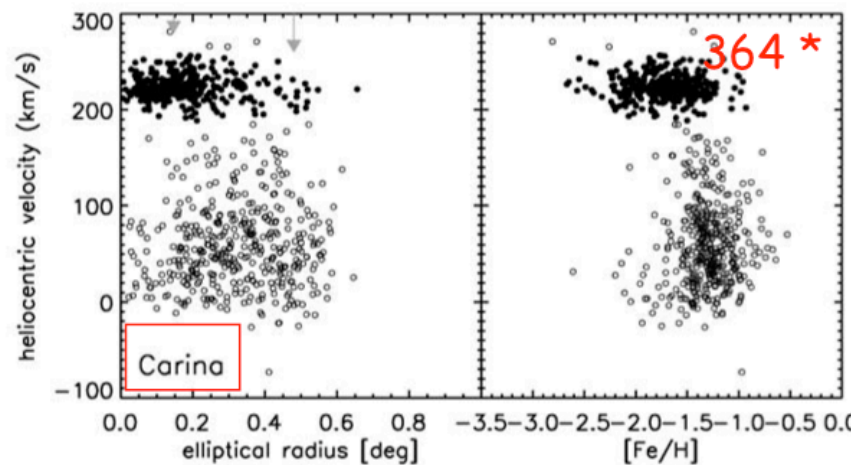
# VLT/FLAMES results



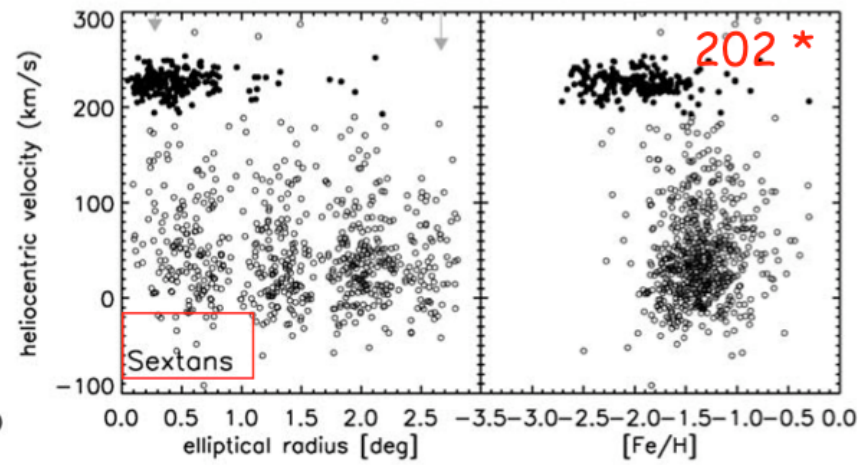
Tolstoy et al. 2004; Battaglia et al. 2007



Battaglia et al. 2006



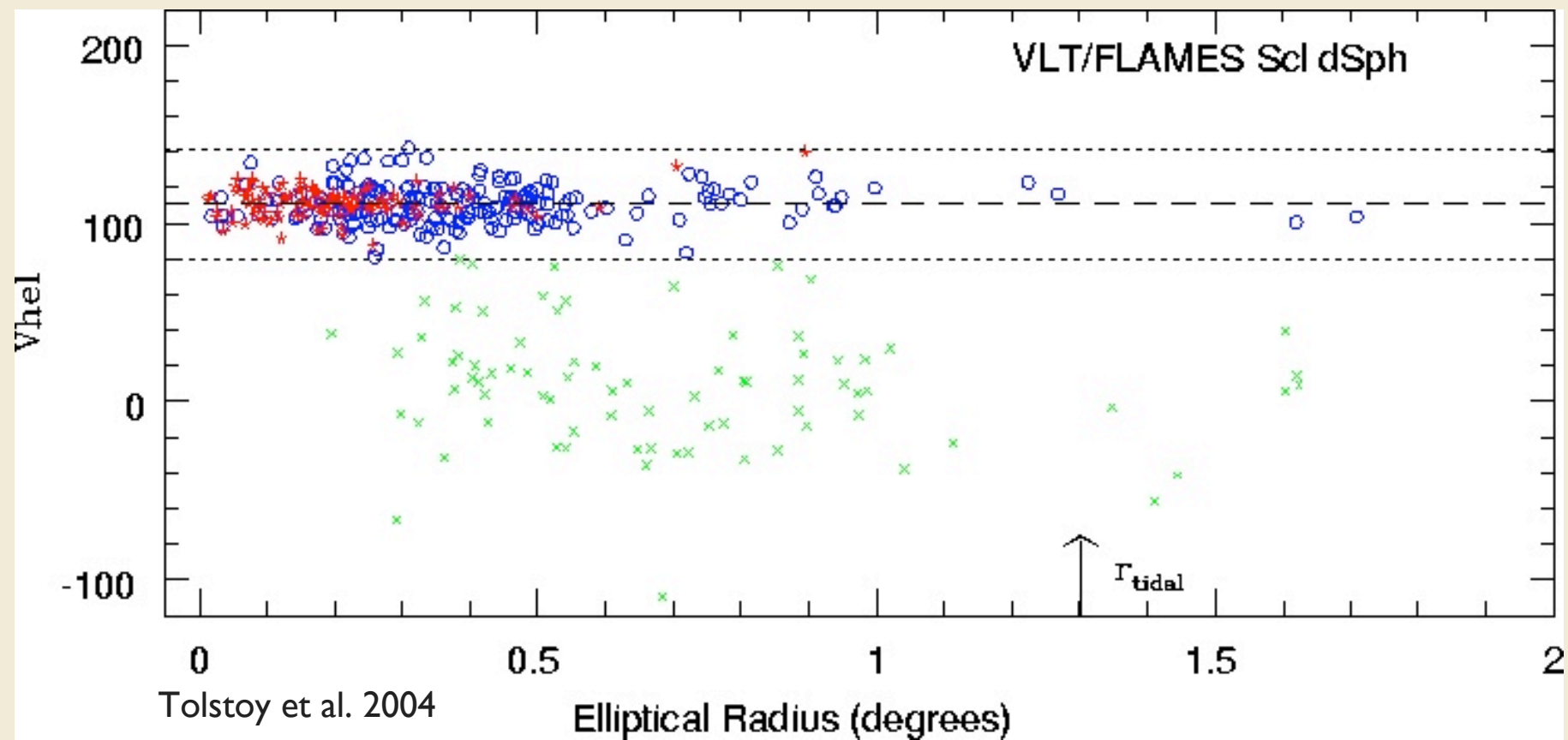
Koch et al. 2006



Battaglia et al. 2007

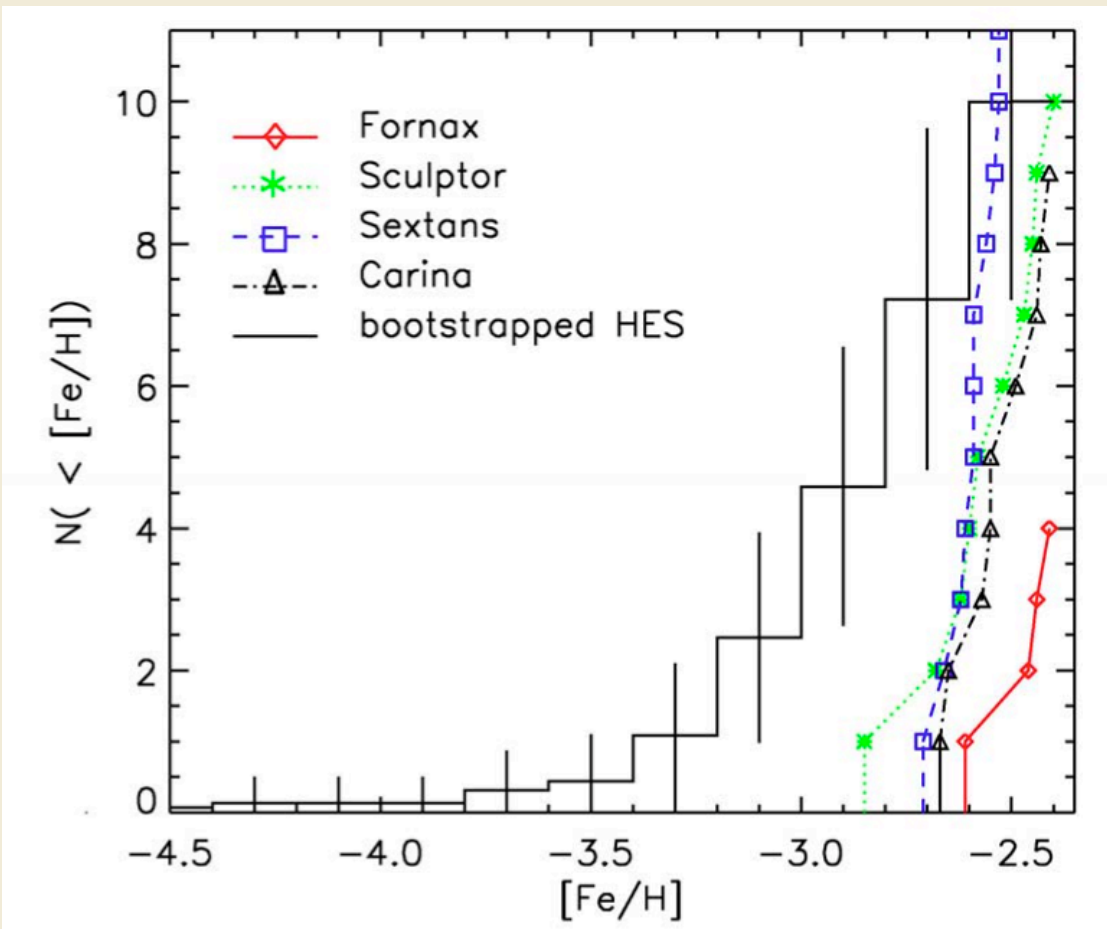


# Kinematics & Metallicity



# No Low Metallicity Tail...

Halo & dSph distributions  
significantly different



If drawn from the same population  
would expect 25%  
of the metal poor stars in  
dSph to have  $[Fe/H] < -3$   
i.e. 35/135

We find no stars  $[Fe/H] < -3$   
(so far)



Helmi et al. 2006, ApJL

# LR spectroscopy cases:

R~5000 resolution spectroscopy in I-band and near-infrared, to measure detailed chemo-dynamical properties in individual stars in galaxies beyond the Local Group.

**-Detailed Star Formation Histories:** in combination with very deep CMDs, spectroscopic metallicities allow to determine an accurate star formation history of a galaxy and put a time scale on chemical evolution. A wide range of galaxy types, will be within reach: spiral galaxies (e.g., NGC253, NGC300, M81) in nearby galaxy groups, such as Sculptor or M81 (2~Mpc away), the closest Elliptical galaxy (Centaurus A, 3.5Mpc away) and also dwarf elliptical galaxies.

**-Chemo-dynamical analyses:** combining kinematic and basic metallicity properties of individual stars allows us to disentangle the dynamical state of a galaxy very precisely accurately. On ELT can go deeper into dense regions than ever before.

The most important wavelength range for these cases is 830nm-880nm, where the Ca II triplet can be found. It has been shown to be an excellent indicator of [Fe/H]. Of course kinematic studies can be carried out where ever there are absorption lines, and perhaps a metallicity surrogate can be found at redder wavelengths - but not happened yet.

# LR spectroscopy: requirements

MOS: >1000 stars per galaxy; 830-880nm or 480-550nm ; R~5000

$$M_i > -4$$

IFU and/or multi-fibres ?

# Resolved Low Mass Stars

High spatial resolution - sensitivity -  
photometric accuracy

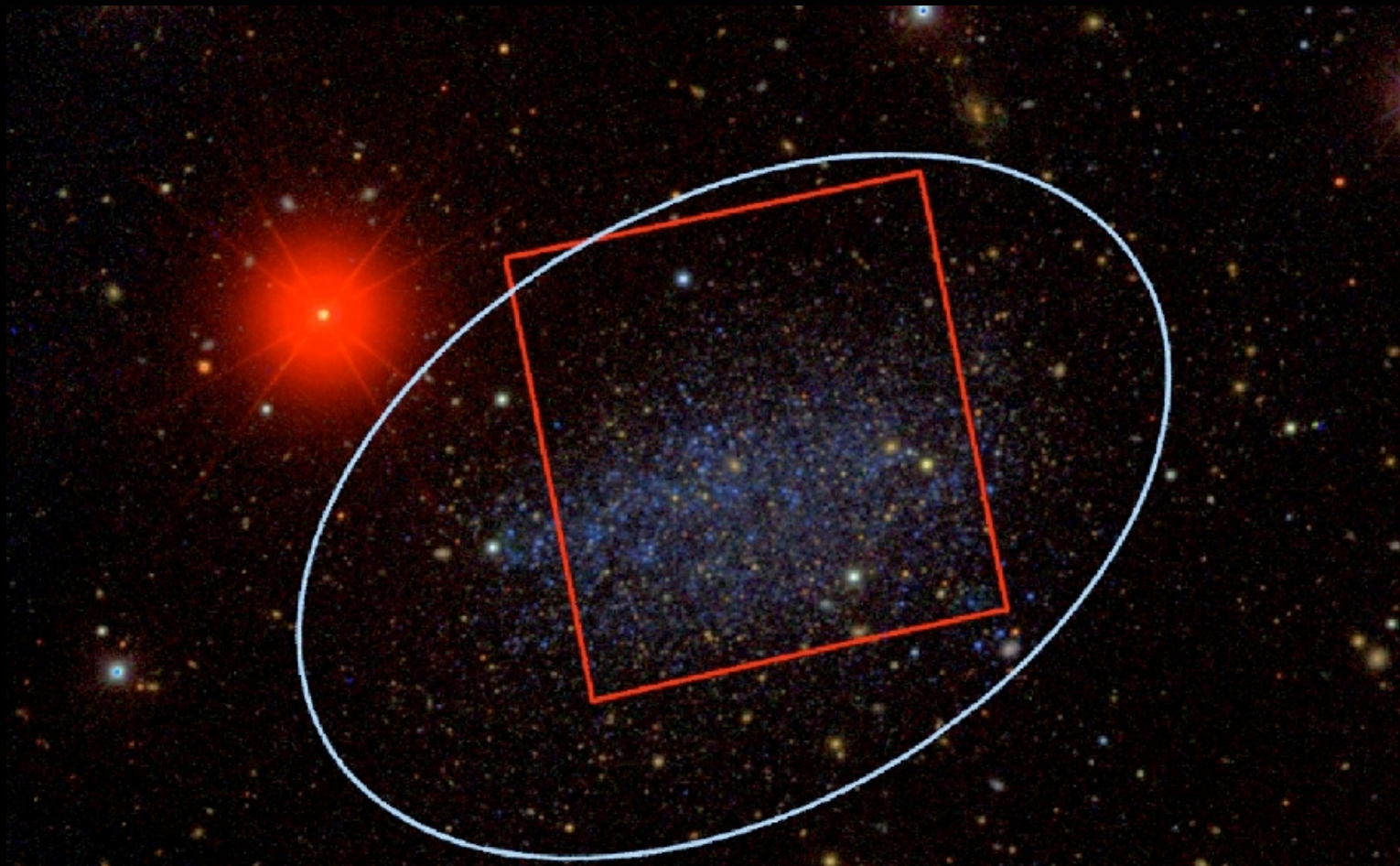
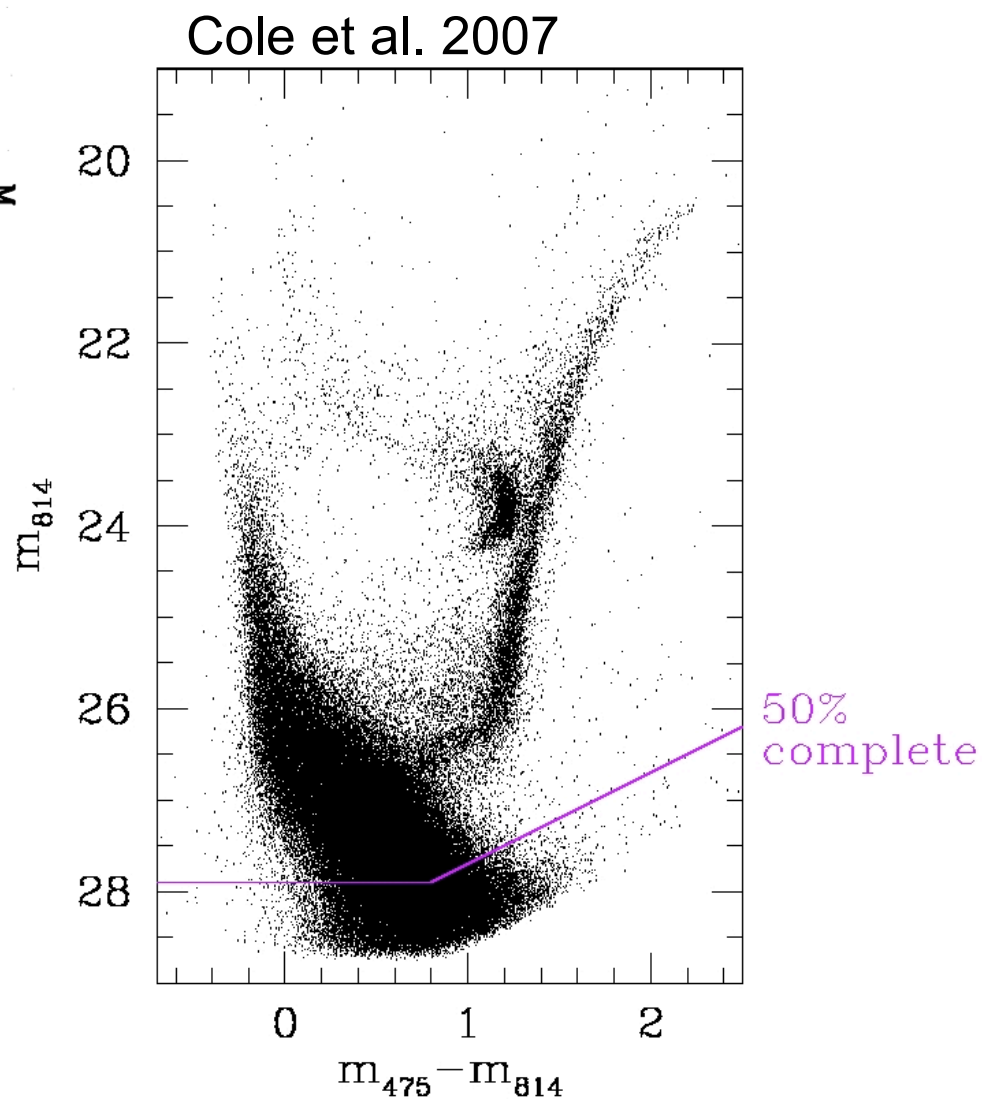
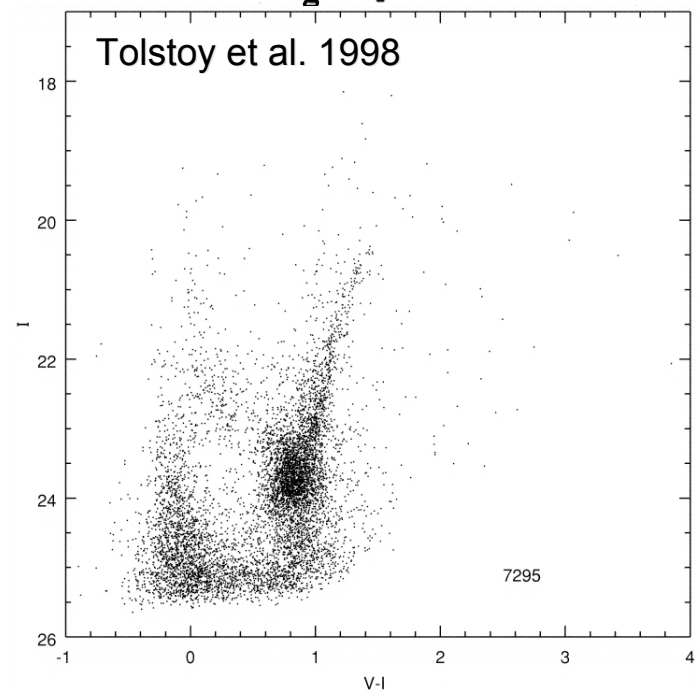
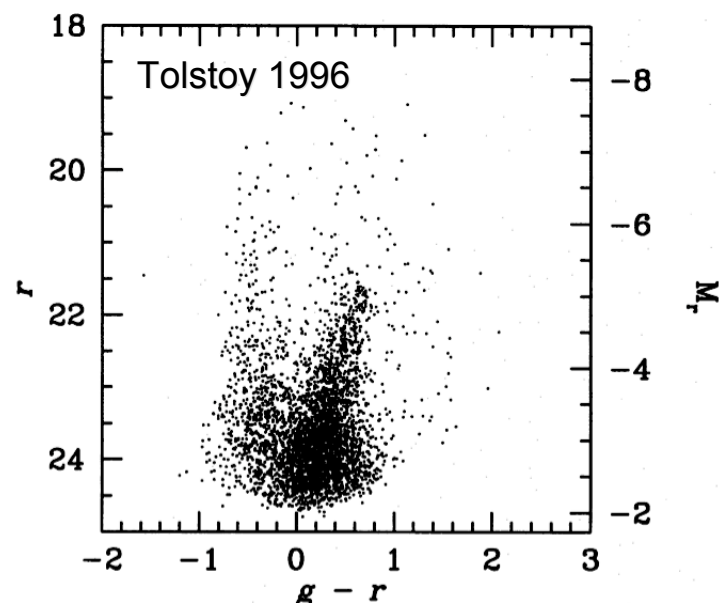
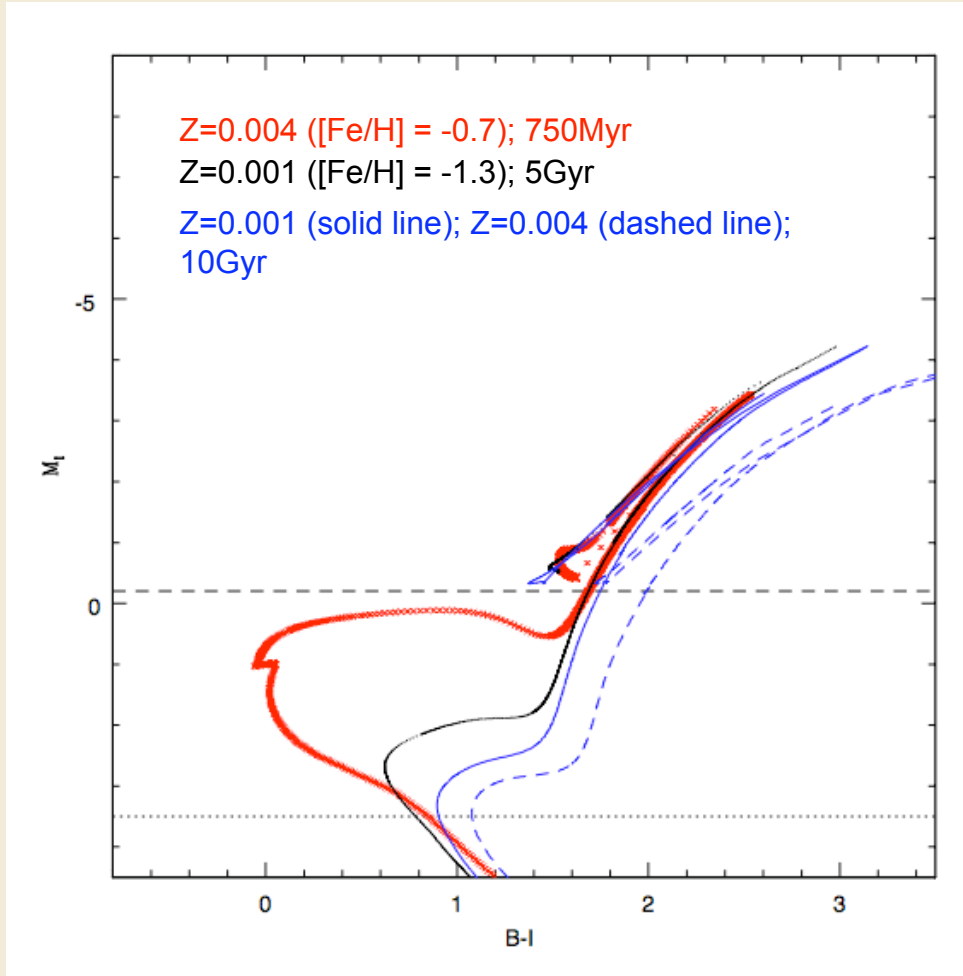
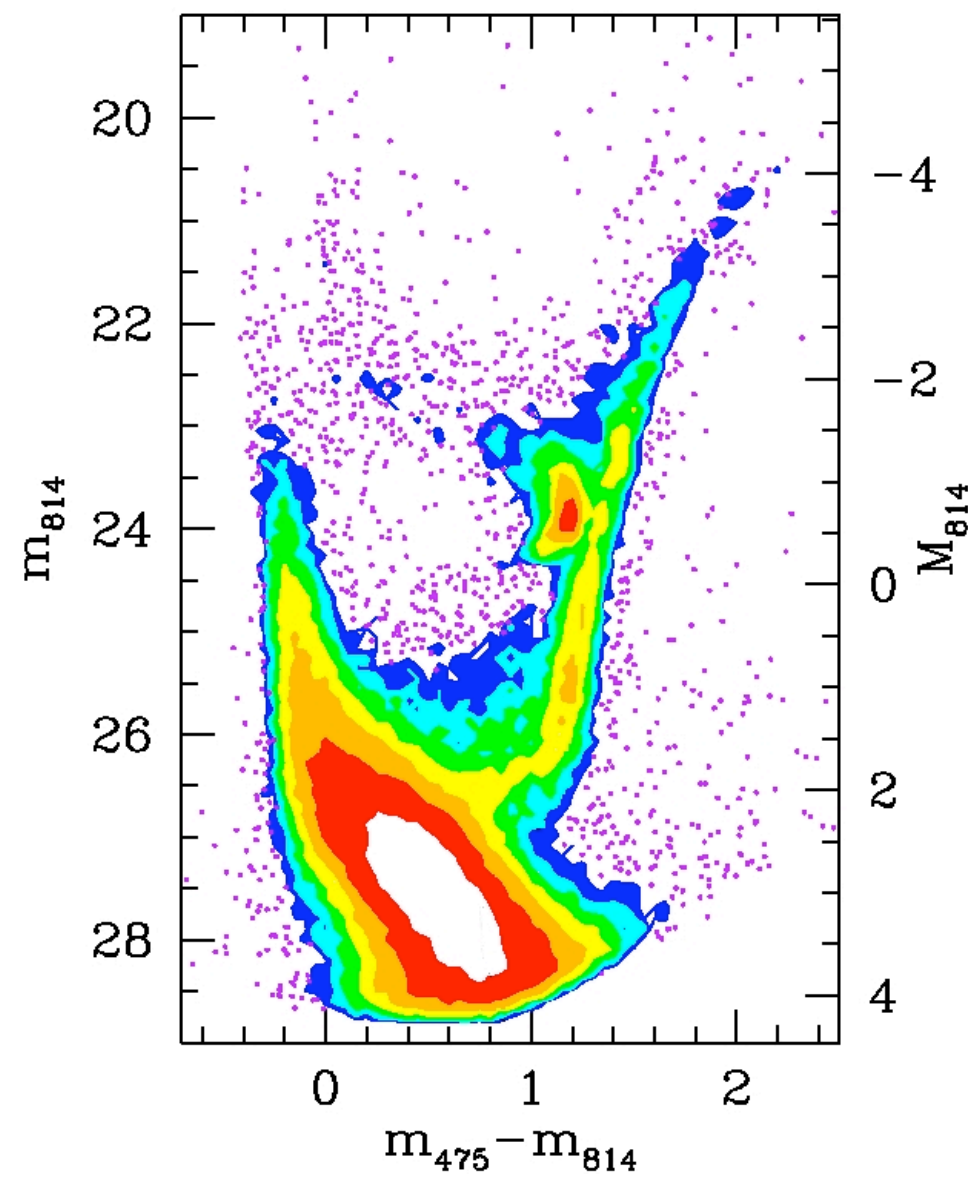


Image: SDSS gri composite.      Ellipse: Holmberg dimension.      Square: ACS



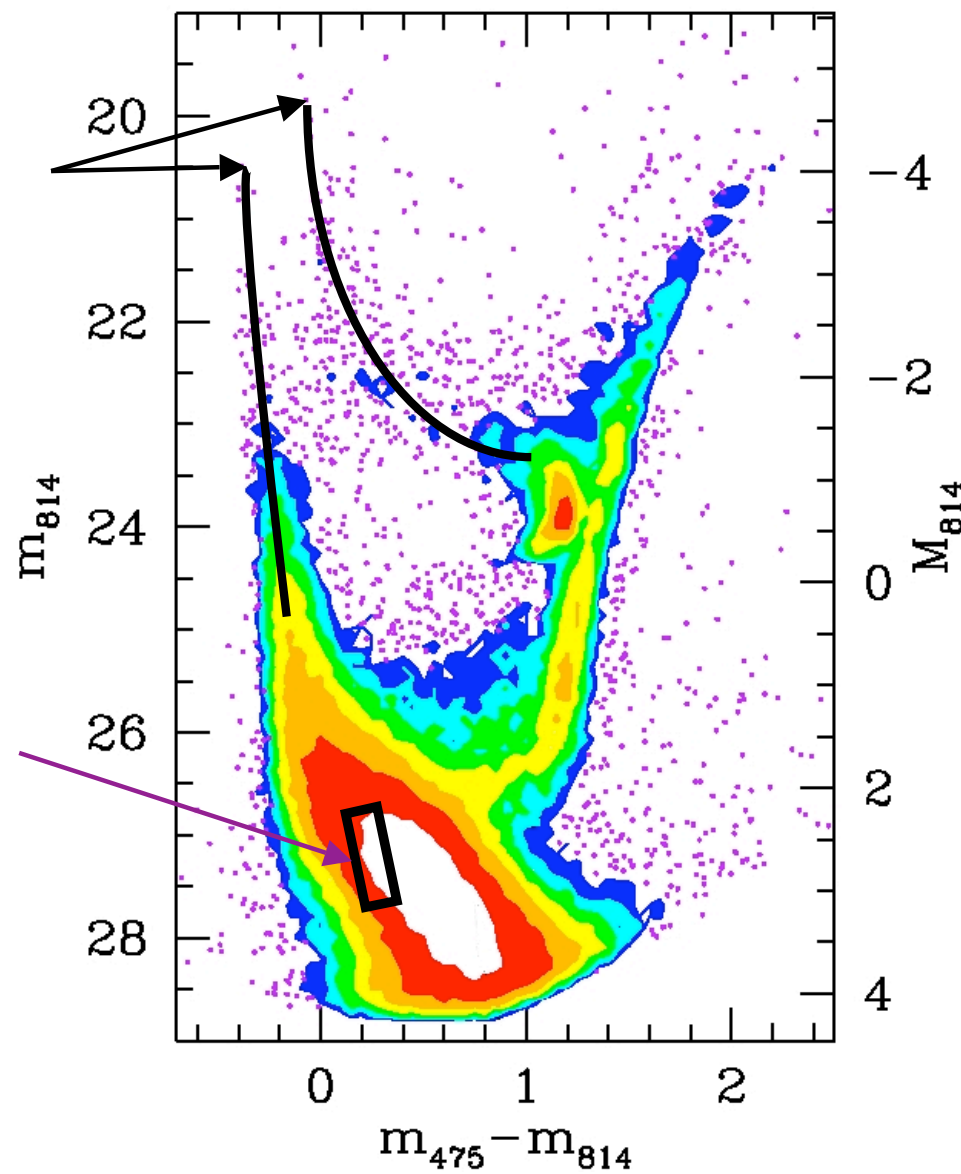
# Age-Metallicity Degeneracy





Main Sequence and Core  
He burning,  $t > 15$  Myr

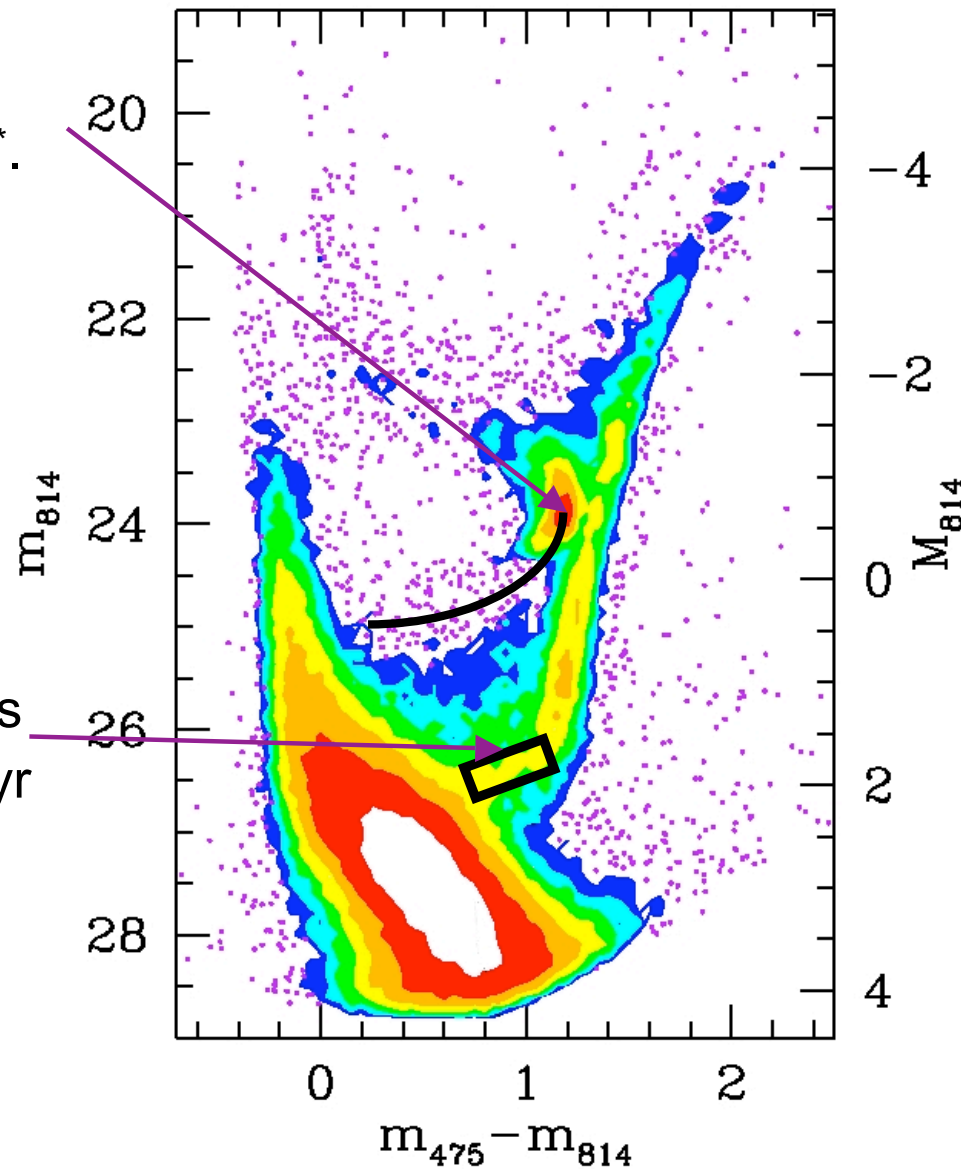
Oldest MS turnoffs,  
6-13 Gyr



Strong red clump, no serious horizontal branch\*.

\* 8 candidate RR Lyraes have been found (Dolphin et al. 2002); we hope to find more in our data.

Peak density of subgiants at similar  $M_I$  as in 2-6 Gyr old Small Magellanic Cloud star clusters.



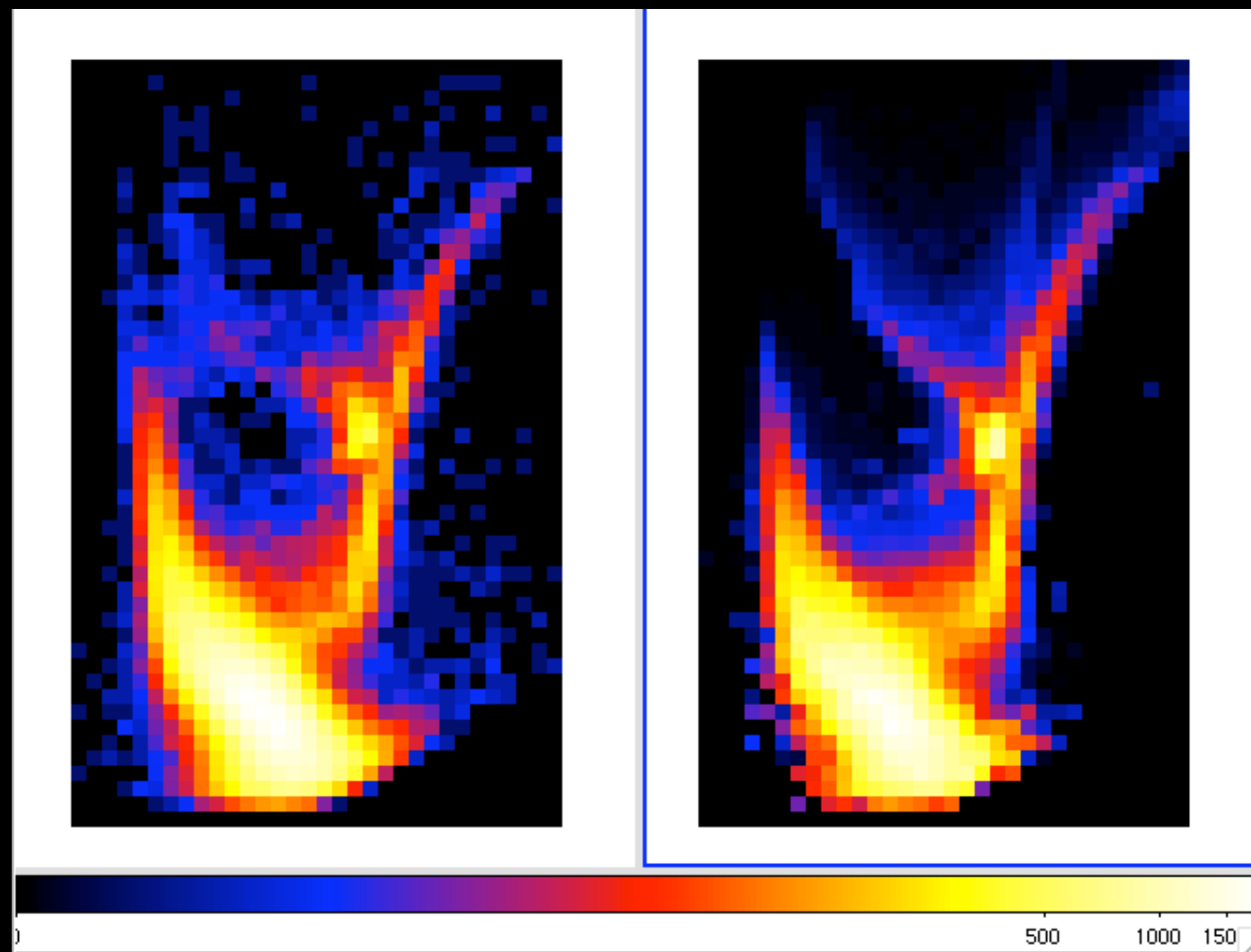
# Analysis: Quantifying the Star Formation History

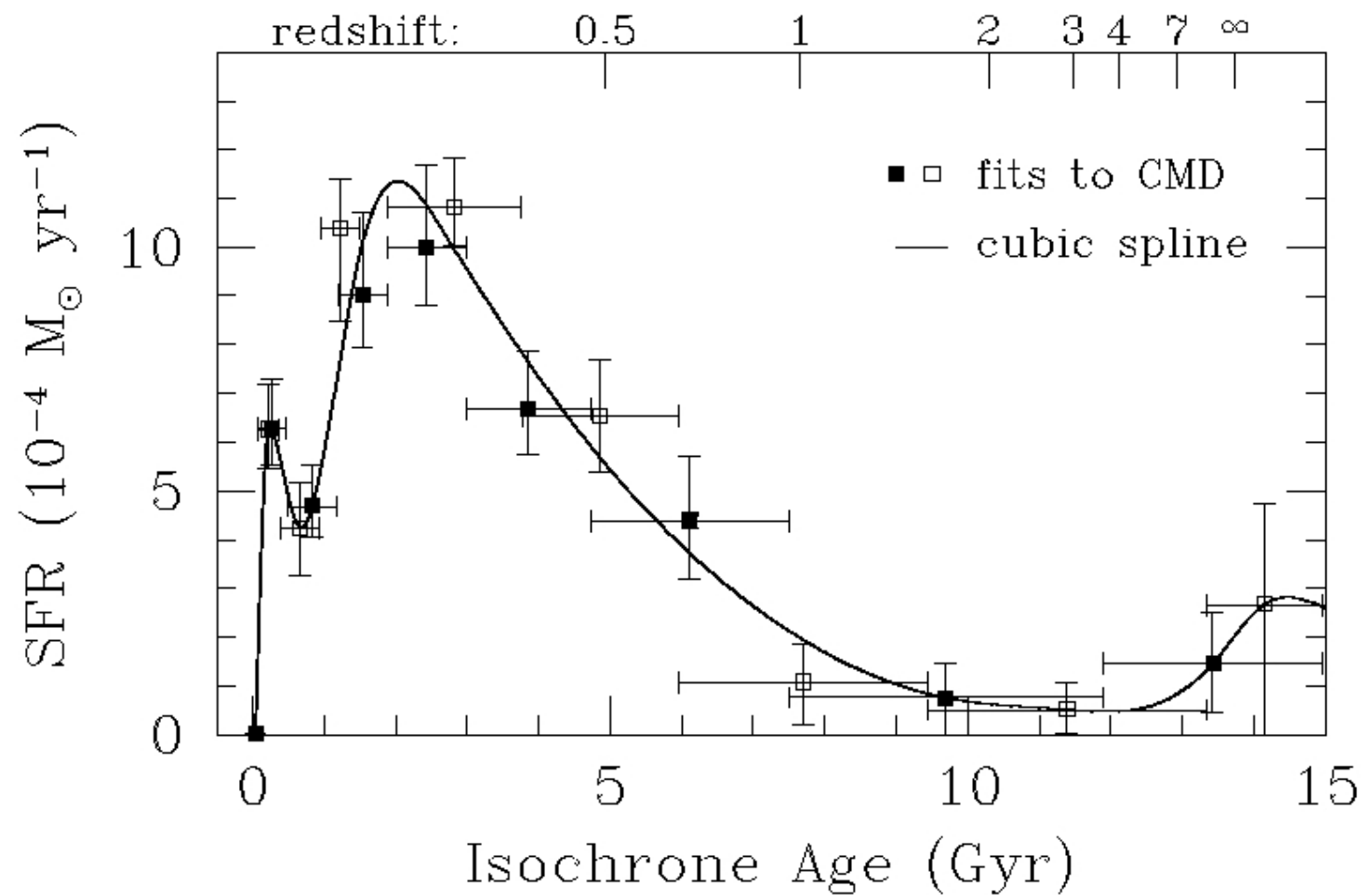
- Compare the photometry to the positions of stellar isochrones at given distance, reddening, IMF, binary star fraction, etc.
- Use a maximum-likelihood technique to determine the distributions in age and metallicity that best recreate the observed CMD.

Observed

CMDs

Synthetic





Results for 2 age binnings, with  $1\sigma$  random errors on SFR

# Choosing filter combinations

ngc55 m-M= 26.3 (1.8Mpc)

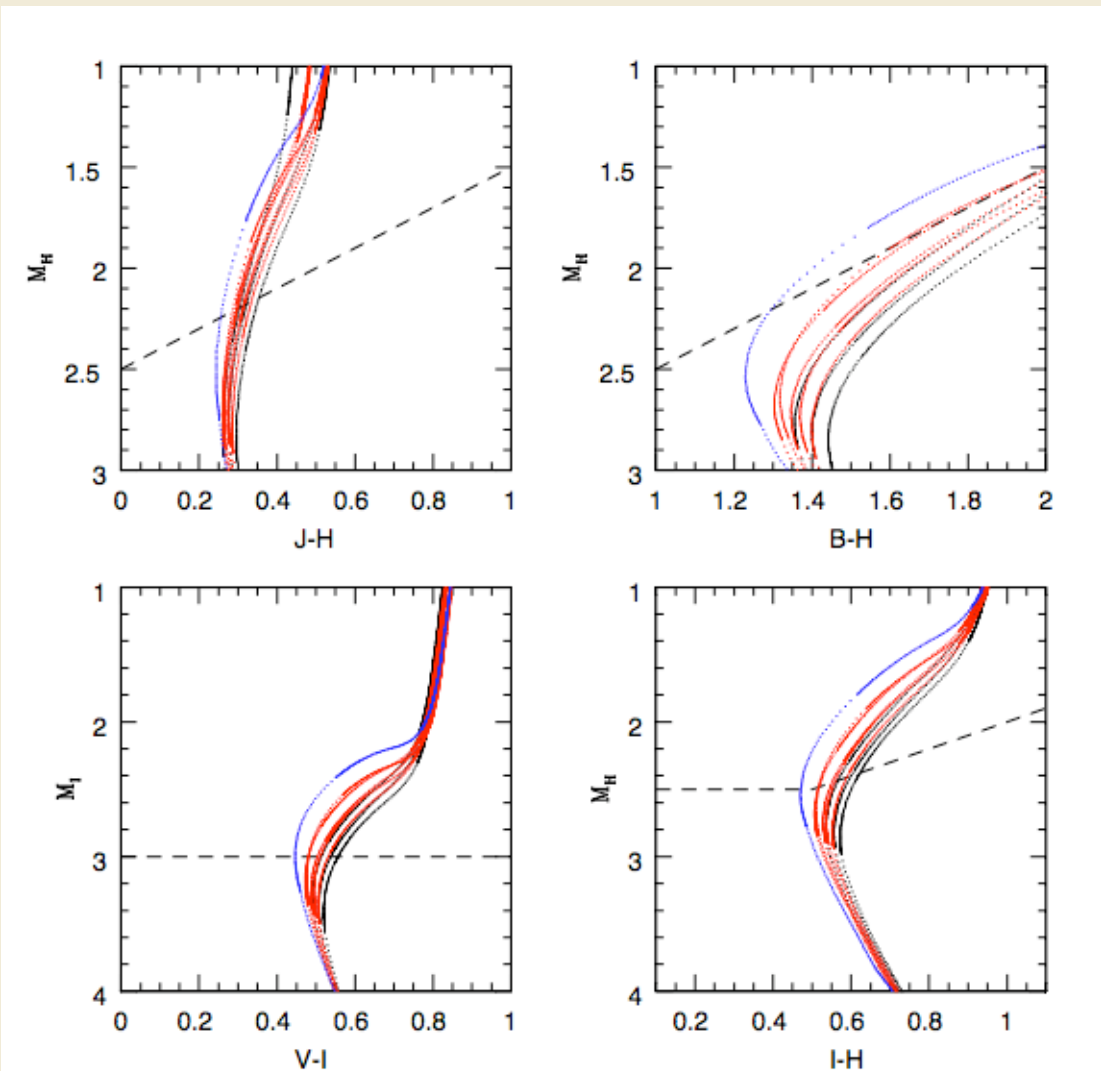
NGC3379 m-M= 30. (10Mpc)

M81/Scl m-M= 27.7 (3.5Mpc)

M31 m-M= 25. (1Mpc)

Depth in 10hrs of integration at S/N~5  
at a distance of 1.7Mpc (HST)

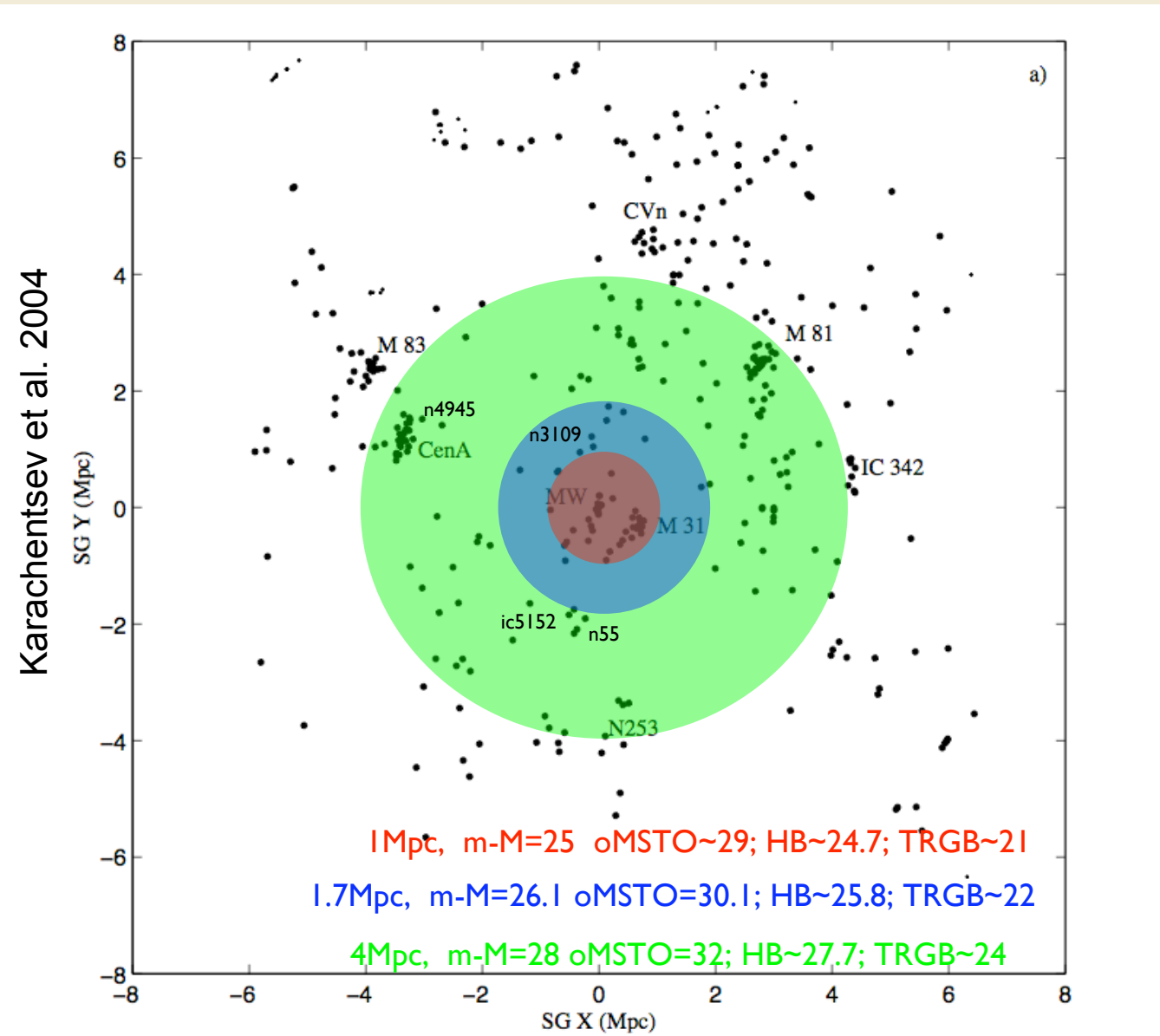
Teramo Isochrones for an low metallicity  
dwarf-type galaxy, range of age ( $>8\text{Gyr}$ )  
and Z ( $[\text{Fe}/\text{H}] = -1.3 \Rightarrow -2.3$ )



10'' at 17Mpc ( $m-M=31.2$ ), is 820pc (equiv. to 4' fov in LG)

Need at least 100 stars per region of the CMD that needs to be modeled, e.g., to get 100 RGB stars need to look at a surface brightness of ~27 with a 10'' fov at virgo.

# Local Group out to 8Mpc



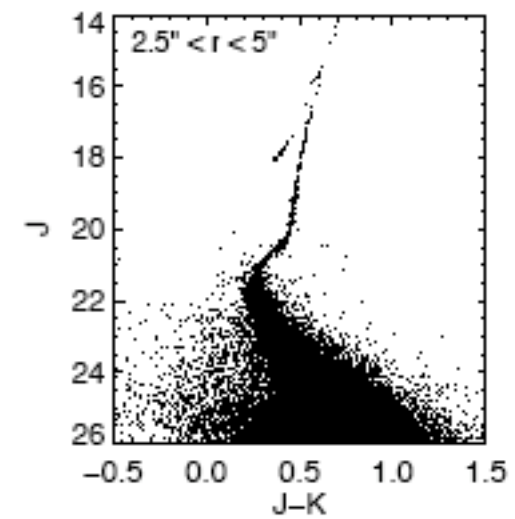
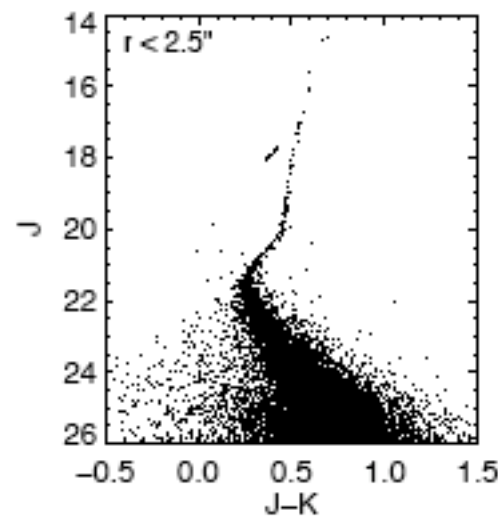
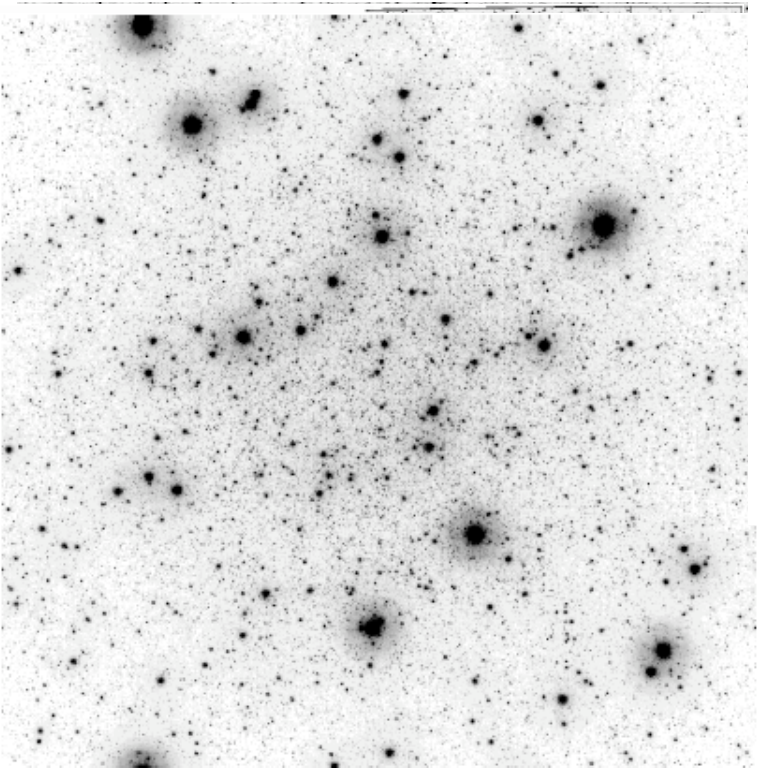
# Trade-Offs

Field of View (fraction of galaxy; size of detector)

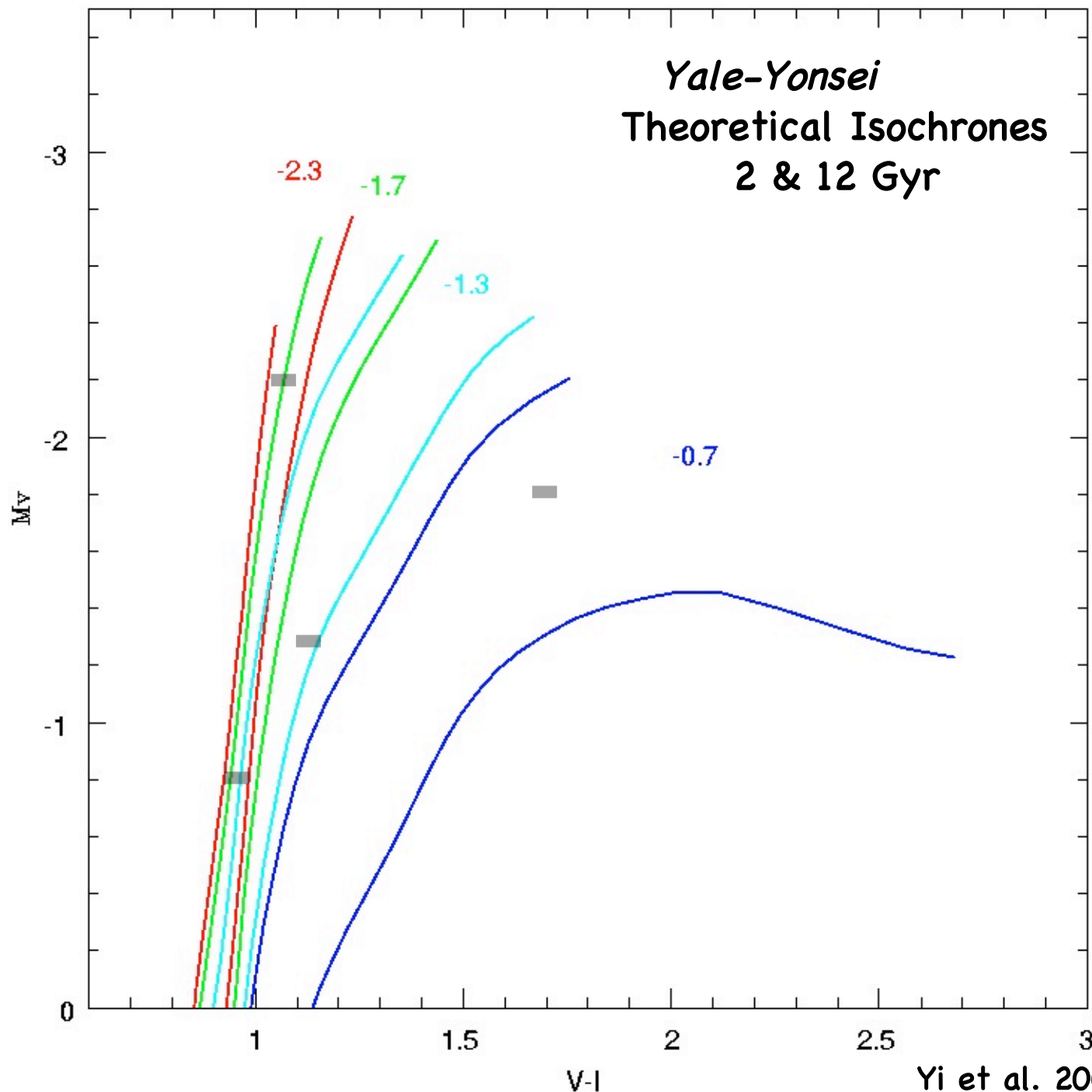
Pixel Size (resolution; diffraction limit; surface brightness limit)

Sensitivity (MSTO, HB, TRGB, E-AGB, young massive stars)

# Crowding



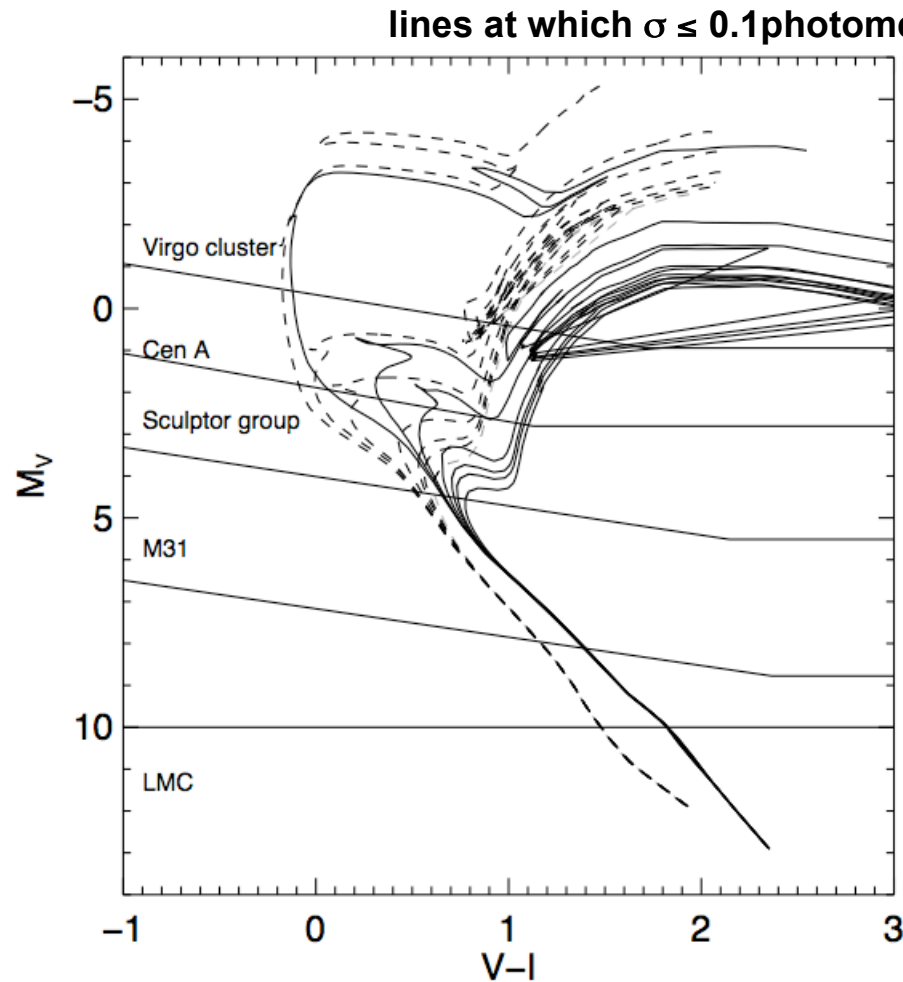
Olsen, Blum & Rigaut 2003



Yi et al. 2003

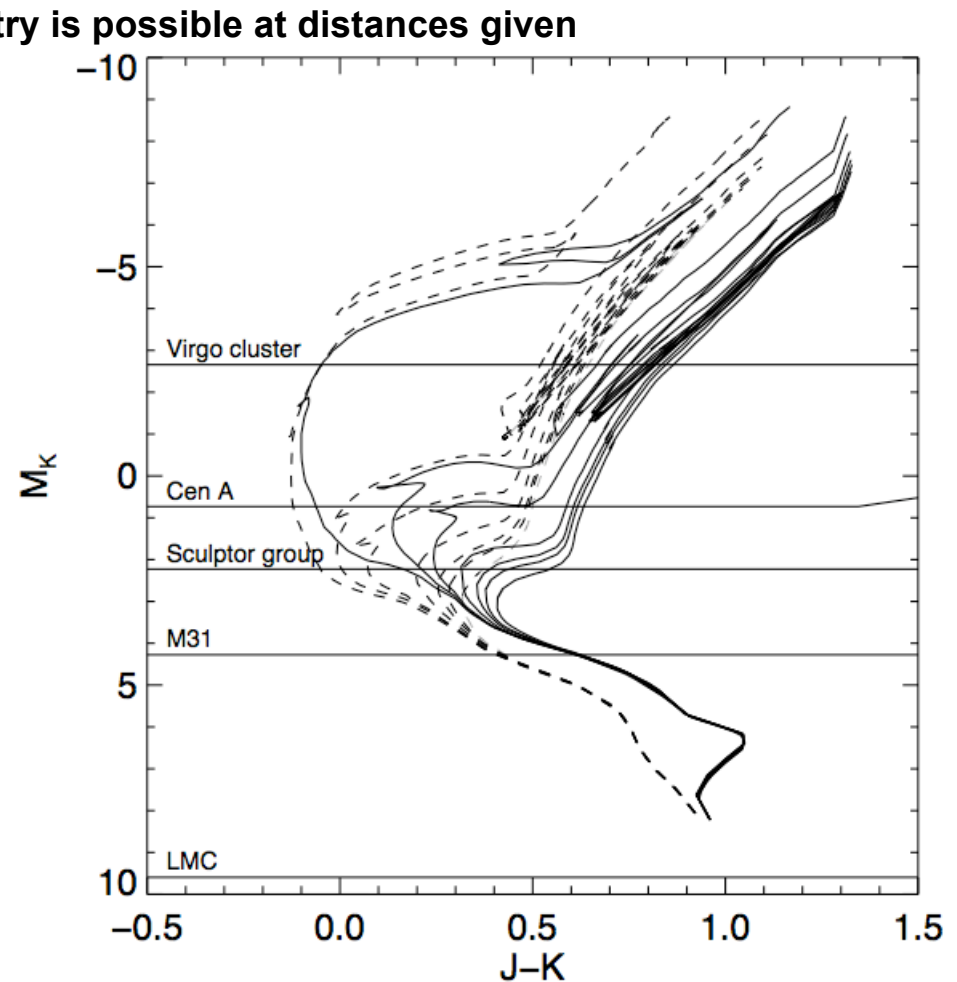
# Optical vs. Infra-Red

30m, diffraction limited telescope



$$\Sigma_V = 22; \Sigma_K = 19; 14 \text{Gyr old}; [\text{Fe}/\text{H}] = -1$$

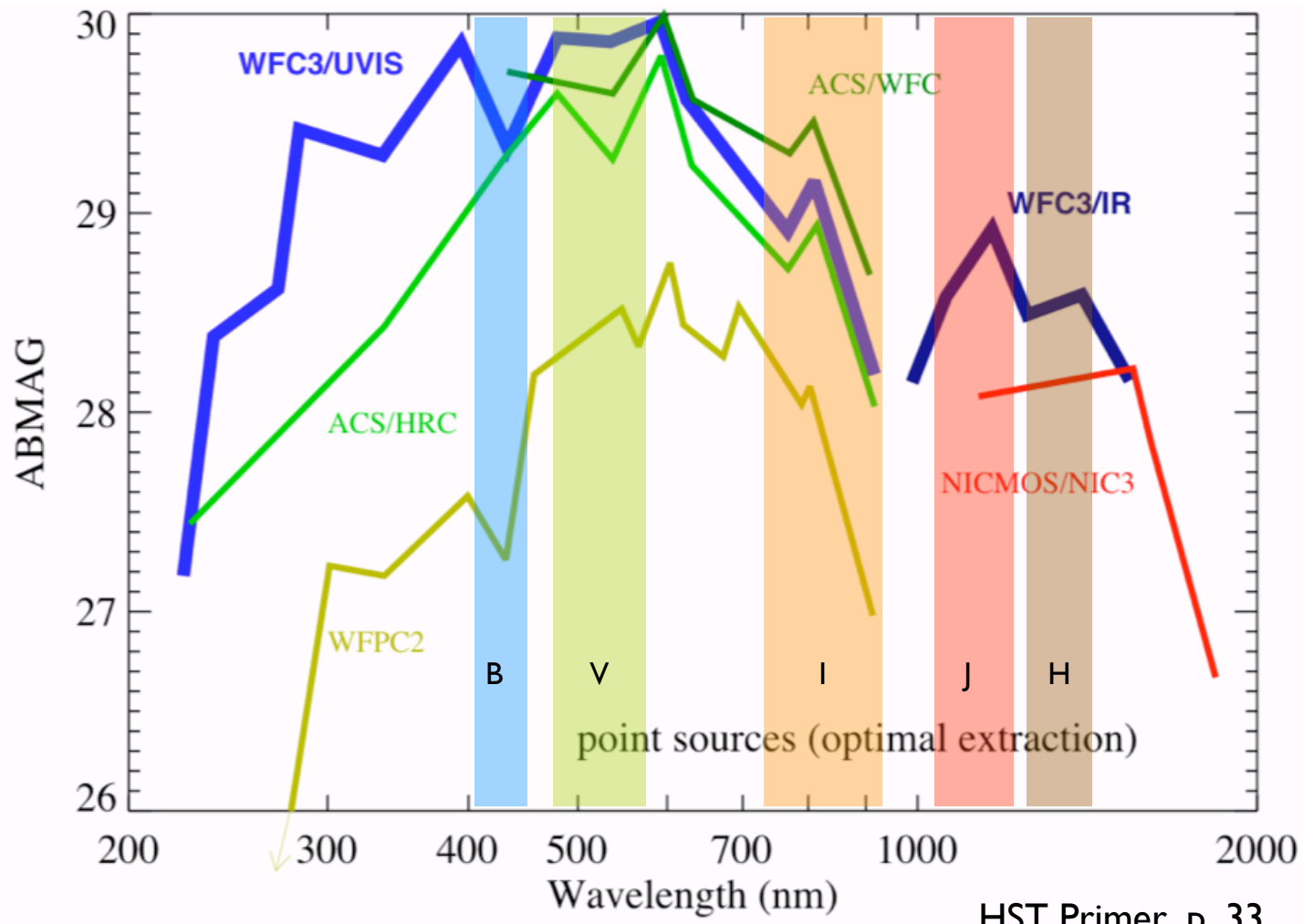
100m, diffraction limited telescope



Olsen, Blum & Rigaut 2003

# *Point Source Limits after SM4*

Figure 4.3: Point-Source Limiting Magnitude  $S/N \sim 5$ ; 10 hr exposure



HST Primer, p. 33

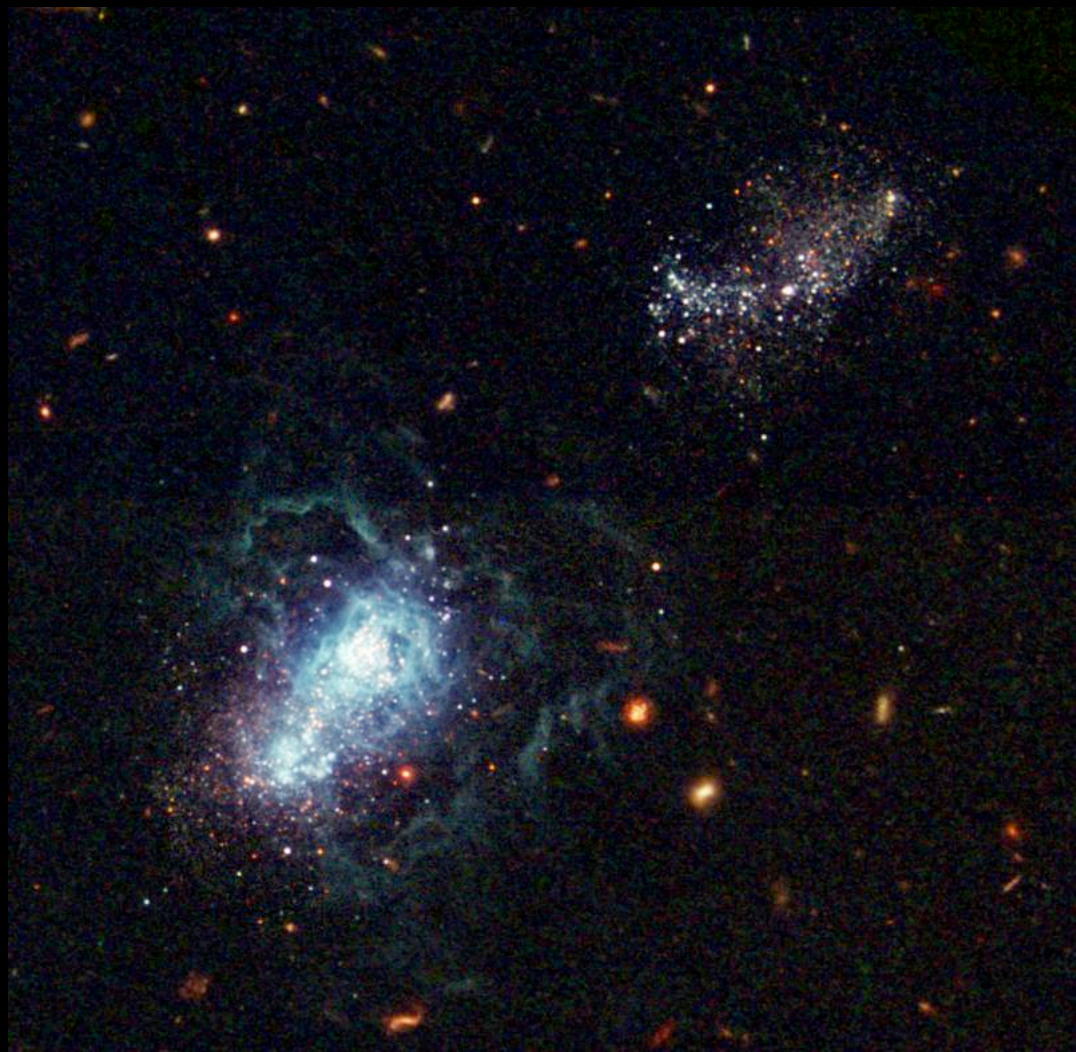
# M59



$I_0 = 15.8 \text{ mag arcsec}^2$

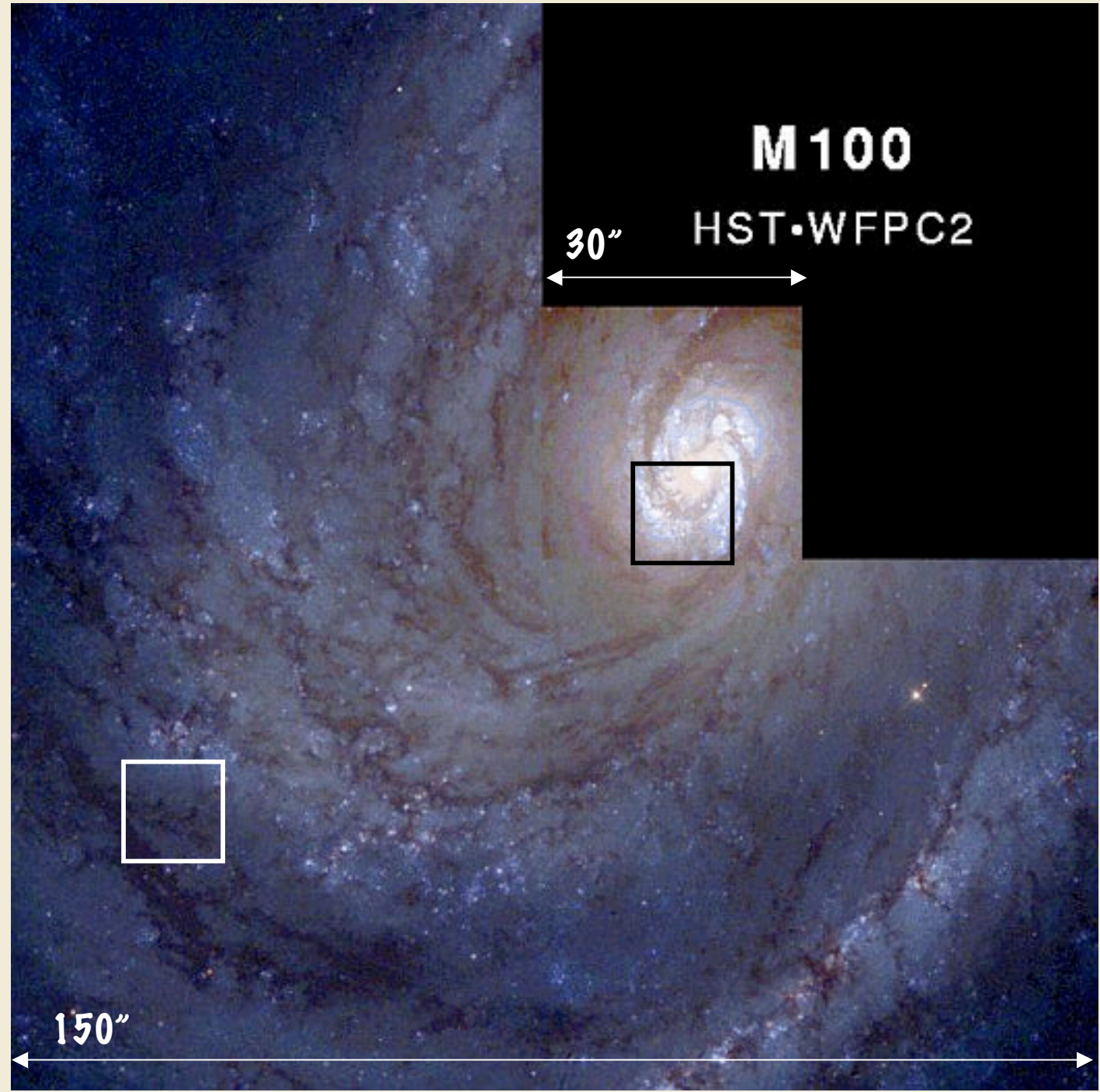
$R_e = 39''$

I Zw 18



2'

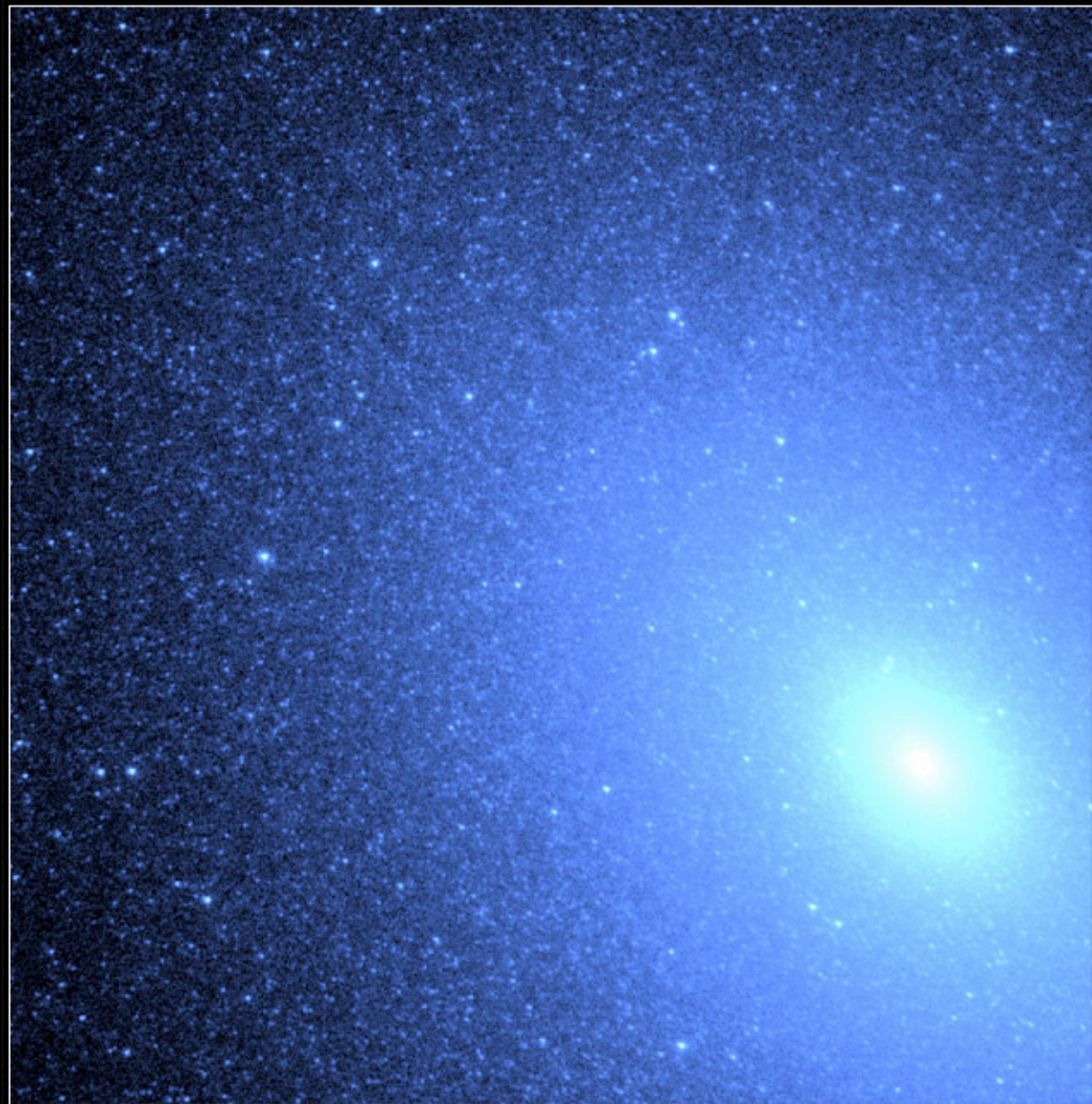
# Virgo Spiral



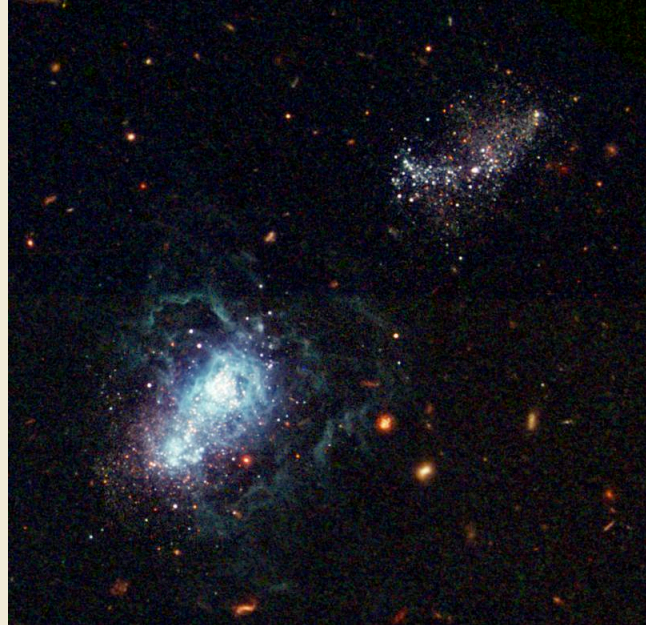
NGC 1569



NGC 1569



HST STIS  
 $24'' \times 24''$



~19Mpc (m-M~31.4)  
24orbits ACS time

I Zw 18

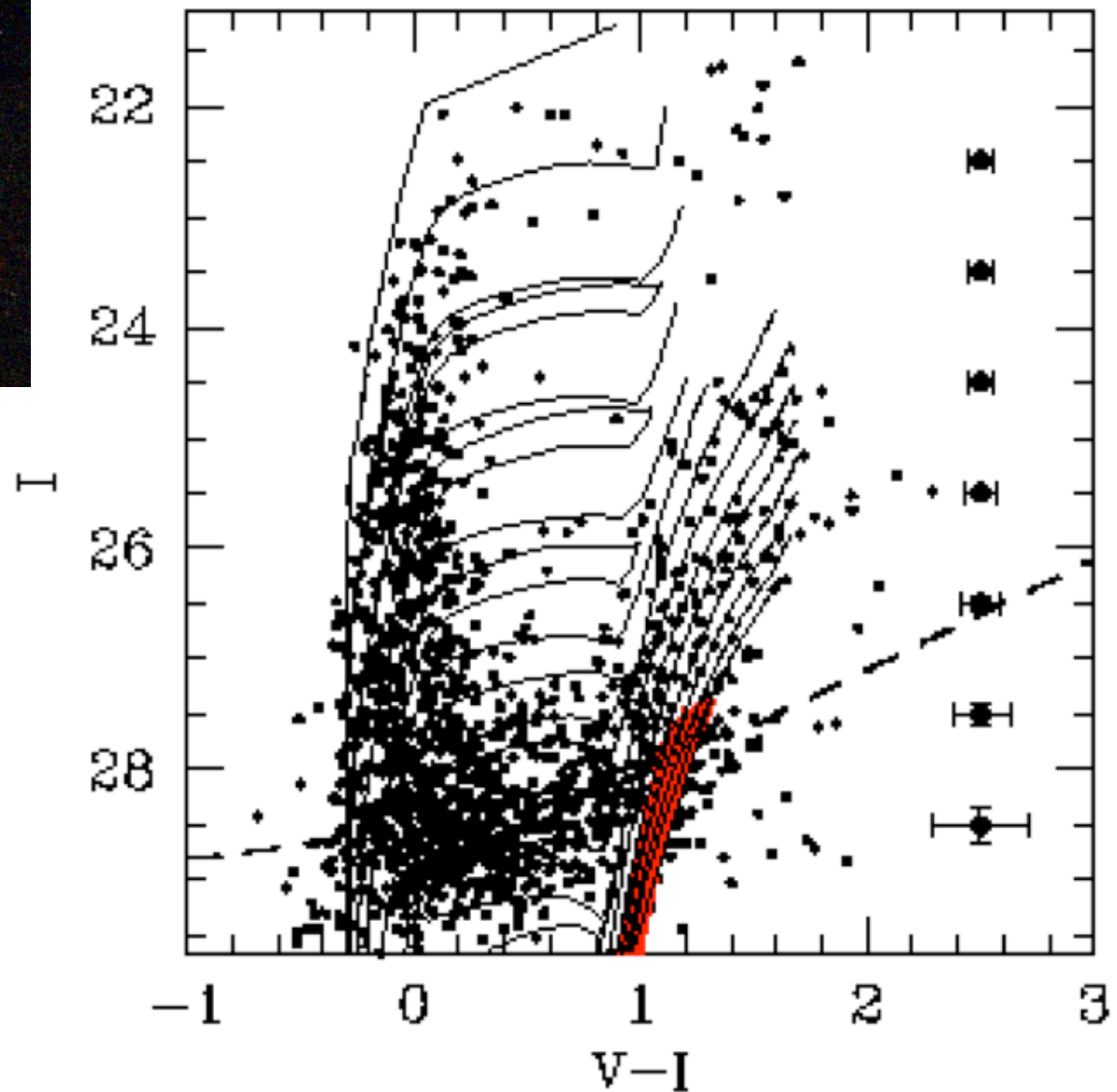


**Table 1.** Potential targets for an ELT

| Object            | (m-M) <sub>0</sub> | θ(1 pc) | Ra(J2000) | Dec    |
|-------------------|--------------------|---------|-----------|--------|
| LMC               | 18.5               | 4"      | 05 23     | -69 45 |
| M31               | 24.3               | 0.3"    | 00 43     | +41 16 |
| Sculptor Group    | 26.5               | 0.1"    | 00 23     | -38 00 |
| M81/82            | 27.8               | 0.06"   | 09 55     | +69 40 |
| Cen A             | 28.5               | 0.04"   | 13 25     | -43 00 |
| Leo Group         | 30.0               | 0.02"   | 10 48     | 12 35  |
| Virgo Cluster     | 31.2               | 12 mas  | 12 26     | +12 43 |
| Fornax cluster    | 32.0               | 11 mas  | 03 37     | -35 37 |
| 50Mpc             | 33.5               | 4 mas   | ...       | ...    |
| Arp220            | 34.5               | 2 mas   | 15 34     | +23 30 |
| Perseus Cluster   | 34.5               | 2 mas   | 03 18     | +41 31 |
| Stephan's Quintet | 35.0               | 2 mas   | 22 36     | +33 57 |
| Coma Cluster      | 35.0               | 2 mas   | 13 00     | +28 00 |
| Redshift z~0.1    | 38.5               | 0.5mas  |           | ...    |
| Redshift z~0.3    | 41                 | 0.2mas  |           | ...    |